Technical

Report

Annual Report
A-B2299-2

SPACE RELATED BIOLOGICAL AND INSTRUMENTATION STUDIES

By

R. J. Gibson
R. M. Goodman

Annual Report
March 1967 to March 1968

Prepared for

NATIONAL AERONAUTICS AND SPACE ADMINISTRATION

Contract NSR-39-005-018

THE FRANKLIN INSTITUTE RESEARCH LABORATORIES
BENJAMIN FRANKLIN PARKWAY • PHILADELPHIA, PENNA. 19103

Technical

Report

Annual Report
A-B2299-2

SPACE RELATED BIOLOGICAL AND INSTRUMENTATION STUDIES

By

R. J. Gibson
R. M. Goodman

Annual Report
March 1967 to March 1968

Prepared for

NATIONAL AERONAUTICS AND SPACE ADMINISTRATION

Contract NSR-39-005-018

THE FRANKLIN INSTITUTE RESEARCH LABORATORIES
BENJAMIN FRANKLIN PARKWAY • PHILADELPHIA, PENNA. 19103

TABLE OF CONTENTS

TABLE OF CONTENTS cont'd.

LIST OF FIGURES

LIST OF FIGURES cont'd.

1.0 ACKNOWLEDGEMENTS

The authors acknowledge contributions to this report via the suggestions, skill, ingenuity and effort of Mr. L. Aruffo, Mr. A. Marmarou, Mr. J. Price, and Mrs. T. Webster

2.0 INTRODUCTION

Pertinent to our studies of the Managed Energy Terrella (MET), we have continued to explore specific techniques of value to the biological researcher. These include the application of loop antennas for use with magnetic induction telemeters, special studies of magnetic shields and field distributions from field generating coils.

Experimental and development effort has continued on the low-cost, high reliability, multichannel implantable telemeter. Particular emphasis has been placed on the evolution of micropower subcarrier oscillators, and substantial progress is reported.

Continued effort has been carried out to improve the characteristics of simple induction-field temperature implants. Specialized probes for deep brain temperature measurement were evolved along with a related telemetry system and receiving, linearizing and recording console.

Useful information exchanges were accomplished by presentation of a paper at the Seventh International Conference on Medical and Biological Engineering in Stockholm and personal visits to the Holly Hill Laboratory of the Medical Research Council in London.

3.0 RECEIVING TELEMETRY SIGNALS BY LOOP ANTENNAS NEAR FIELD

Small implantable telemeters operating in or near the broadcast band (300 KC → 3 MC) utilize the magnetic field coupling to the pickup antennas to transmit information. The oscillating current in the tuned circuit coil of the telemeter generates a magnetic field; this magnetic field cuts the antenna conductors and induces a voltage in them. This voltage is proportional to the number of magnetic field lines produced by the transmitter, the number of conductors in the receiving antenna and the frequency of the carrier signal. If one assumes that a uniform field is generated by the transmitter, then the voltage produced is a cosine function of the angle between the planes of the transmitting antenna and the receiving antenna. However, even this simple assumption cannot be made since at a distance around ten times the diameter of the transmitting coil the field is far from uniform and is more nearly that of a magnetic dipole. In addition, the receiving antenna is generally one to two orders of magnitude longer than the transmitting antenna. See Fig. 3.0-1.

Further, the transmitting antenna may be at almost any distance from the receiving antenna as well as at any orientation to it. For these reasons, it is generally quite complicated to determine theoretically just what signal is to be expected from the receiving antenna in the general case. Theoretical calculations can, however, be most useful in deriving design approximations. These approximations

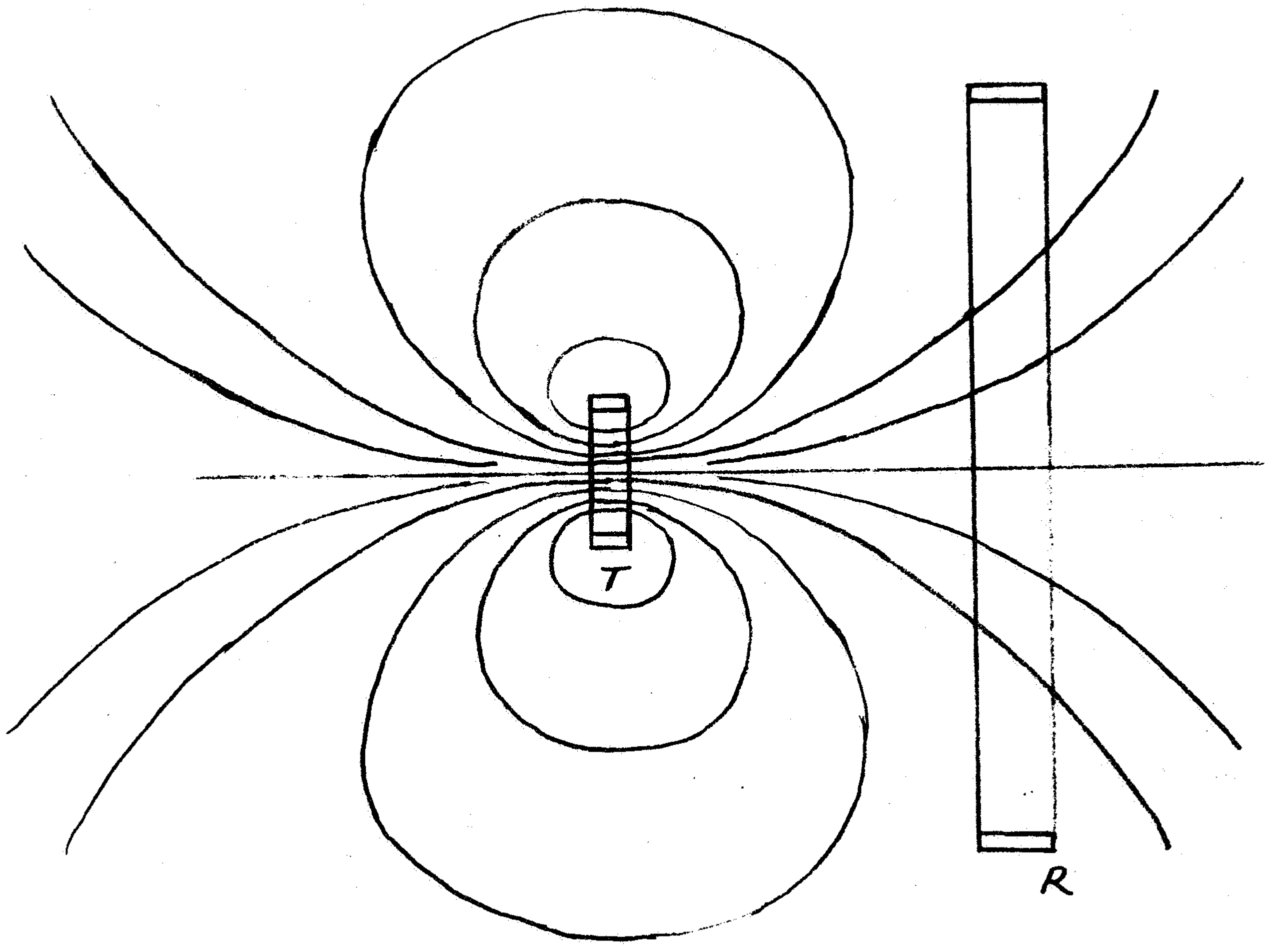

FIG 3.0-1 FLUX LINES FOR TRANSMITTING (T) AND RECEIVING ANTENNAS (R).

have led to the design of tri-orthogonal systems for the general case (3-1). Also see loop antenna approximate calculations in (3-2, 3-3, 3-4, 3-5). Actual measurements of the received signals for various configurations of geometry between transmitting and receiving antenna and relative sizes and geometry of the receiving antenna were considered to be necessary to determine the limits of useful size and shape of receiving antennas. In particular, this information was required for the Mark IV telemeters and antennas on the order of a few feet in diameter. Various practical considerations such as construction difficulties, cost, cage access, tri-orthogonal configurations, etc. lead us to receiving antenna shapes and sizes as follows:

1. Square or nearly square rectangular antennas
2. Fewest possible turns
3. Spacing on the same order as the dimension of the antenna side

Item 2 was dictated by the fact that it was desirable to have a small self-capacitance of the antenna loop so that its inductance could be tuned to the carrier frequency of the transmitted signal. Tuning of the antenna is desirable in that the signal at the antenna terminals can be increased by <u>one or two orders of magnitude</u> depending on the Q and loading of the antenna. Tuning also is quite effective in reducing the relative response of the antenna to constant frequencies below and above the tuned frequency, but has little effect on pulse or spike noise inasmuch as the resonant circuit is shocked by noise of this type to resonate at the carrier frequency. Pulse or spike noise is most difficult to eliminate but progress has been made in that direction by the use of fixed gate or dynamic gate receivers (3-5).

MEASUREMENTS

Antenna frames 2 x 2, 3 x 3 and 4 x 4 feet square were constructed of $\frac{1}{2}$" thick white pine lumber. These were wound with the desired number of turns of No. 25 plastic insulated wire. A few antennas were constructed using No. 28 enameled wire, but no difference due to wire size and insulation could be detected. Antenna turns spacing were 1/8", $\frac{1}{4}$' and $\frac{1}{2}$". Tuning was accomplished by a capacity box connected to the antenna terminals. Loading to the desired amount was accomplished by a resistance box shunted across the antenna terminals in parallel with the tuning capacitor, Fig. 3.0-2. Loading was 10 kilohms in most measurements to simulate a typical reciever load. Most antennas were loaded to $\frac{1}{2}$ amplitude by approximately 2 K ohms to 5 K ohms. Amplitude of signal was determined with a high gain oscilloscope. Signal measured is expressed in peak-to-peak voltage. Inductance measurements were obtained with a Wayne Kerr Universal Impedance Bridge B221A with a Type Q221A Low Impedance Adaptor at 1592 cps. Series inductance and resistance was computed from measured parallel inductance and resistance. Where two antenna frames were used, the connections were such that the signals were aiding. RG 174/U miniature coaxial cable was used to connect the antenna to the measuring oscilloscope. This cable had a measured capacity of 33 $\mu\mu$ fd per foot.

A standard Mark IV telemeter was used as the signal source for most measurements. For the large antenna (4' x 4') a high power

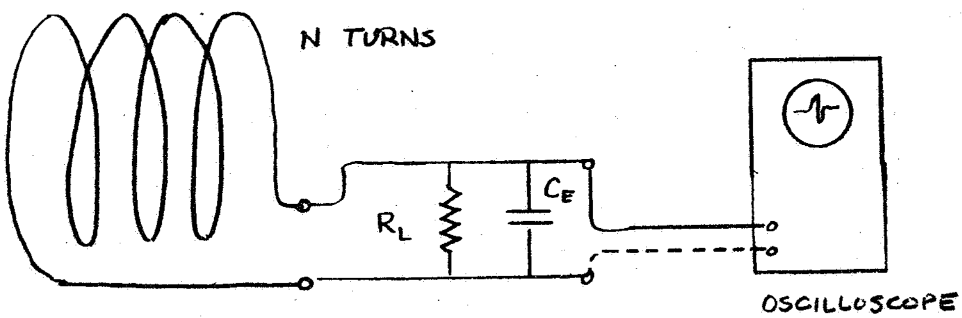

R_L = ANTENNA LOAD
C_E = TUNING CAP.

FIG 3.0-2 ANTENNA MEASURMENT SYSTEM

breadboard telemeter was used, but values were corrected to the Mark IV level.

NUMBER OF ANTENNA TURNS VS. SIGNAL LEVEL

Fig. 3.0-3 and the table show a typical curve of the increase of signal strength as the number of turns is increased. This is for a 2' x 2' antenna, but other antenna sizes and spacings are very similar. The expected signal strength should increase as the straight line in the figure or as the calculated relative values in the table. As can be seen from the figure, above about 5 or 6 turns each additional turn adds less than expected of it. In each case the load was high ($\sim$ 10K) and the number of turns was tuned to give maximum signal.

ANTENNA TUNING CAPACITANCE, EXTERNAL

In order to obtain a better signal-to-noise ratio and to increase the signal level it is desirable to tune the antenna inductance with an external capacitor to the carrier frequency of the telemeters, which is about 500 KC. Tuning of the antenna attenuates other carrier signals passing through the antenna area both above and below the tuned frequency and increases the carrier signal by approximately the Q of the tuned antenna. The antenna has a distributed capacitance which increases rapidly as the number of turns increases. Since any capacitance of the cable connecting the antenna to the receiver acts itself as a tuning capacitor, it is necessary to take this into consideration. The self-capacitance is such that a very small external capacitance is required for tuning. This may prohibit a long run of such cable to the receiver.

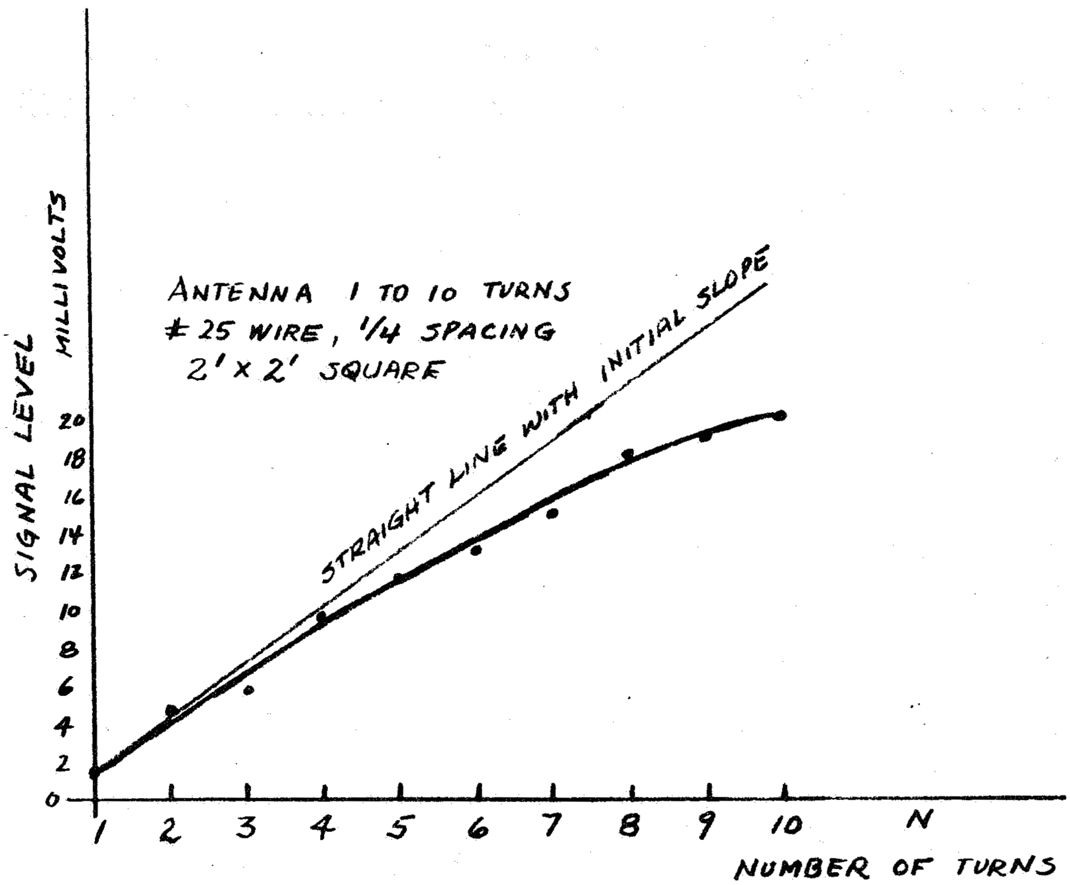

FIG 3.0-3 RELATION BETWEEN SIGNAL STRENGTH AND NUMBER OF TURNS FOR A TUNED ANTENNA.

Table for Fig. 3.0-3

N Number of Turns	Signal Level pp (mv)	Relative (to 10 turns) Signal Level	Calc. Rel. Signal Level
1	$\simeq$ 1.5	.8	1
2	5.0	2.8	2
3	5.5	3.1	3
4	9.6	5.3	4
5	11.5	6.4	5
6	13.0	7.2	6
7	15.0	8.3	7
8	16.0	8.9	8
9	16.7	9.3	9
10	18.0	10	10

For 2' x 2' square antenna; No. 25 wire, $\frac{1}{4}$" spacing, telemeter at center of antenna

The table below shows typical external tuning capacitance required for single frame antenna in sizes and turn spacing shown for various number of loop turns.

(Length x width; turns spacing)

Antenna	2' x 2'; $\frac{1}{4}$"	3' x 3'; $\frac{1}{2}$"	4' x 4'; 1/8"	4' x 4'; $\frac{1}{4}$"
	External tuning capacitance in μfds			
No. of turns				
1	.030	.022	.007	.014
2	.010	.008	.0022	.0048
3	.0053	.0041	.0008	.0024
4	.0032	.0022	.0004	.0014
5	.0022	.0015	.0002	.0009
6	.0015			
7	.00115			
8	.0009			
9	.00073			
10	.0006			

These are typical values of the required external tuning capacitance. When two frames are used, spaced approximately one frame length apart, and connected in series-aiding configuration the required tuning capacitance is just twice that required for one frame. If two 2' x 2'; $\frac{1}{4}$" antennas were used with five turns each, the C required would be .0022 μfd divided by 2 or .0011 μfd. This value would allow up to .0011 μfd/33μμfd/ft = 33 feet of miniature coaxial cable between the antenna and the receiver, the cable capacitance acting very much like a lumped capacitance.

The relationship between number of turns and the required external capacitance can be fitted fairly well by the equation.

$$C_e = C_o/N^{1.5} - C_r \tag{1}$$

where C_e = external tuning capacitance

C_o = constant

C_r = constant

N = number of turns

all C's in μfds

For most of the antenna tested C_r was approximately .0004 μfd, and C_o was found to be represented very approximately by

$$C_o = 0.23 \left(\frac{S}{D}\right) \tag{2}$$

S = turns spacing in inches

D = frame side in feet

C_o in μfds

For a first "ball park" figure the following equation can then be used as a design equation.

$$C_e \approx \left(\frac{0.23S}{DN^{1.5}} - .0004\right) \text{ μfds for one frame} \tag{3}$$

Where S is in the range 1/16" to 1/2" and D is in range 1 foot to 4 feet. More accurate values for C_o and C_r can then be determined by measurements on the completed antenna and used in equation (1).

ANTENNA INDUCTANCE

Calculation of the antenna inductance is much more accurate and straightforward. Excellent agreement was found between measured antenna inductance and that calculated from Wheeler's modified formula (3-6) given below as equation (4) for a circular antenna, single layer.

$$L = \frac{a^2 N^2}{(9 - \frac{a}{5\ell})\, a + 10\ell} \quad \mu h \tag{4}$$

a = radius in inches

ℓ = length of antenna coil in inches

N = number of turns

for $2a/\ell < 20$

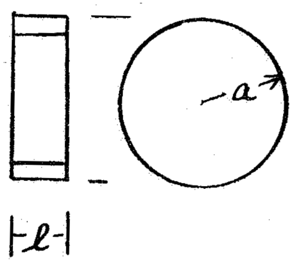

For a square antenna use a value of "a" calculated as in equation (5).

$$a = 1.19 \left(\frac{D}{2}\right) \tag{5}$$

D = length of antenna side in inches

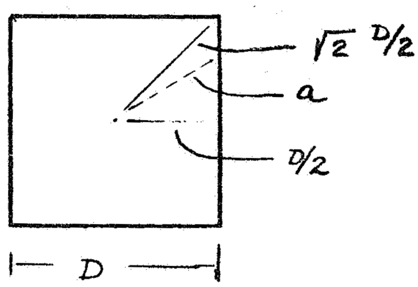

Here the radius is the geometric mean of $\frac{1}{2}$ the side and $\frac{1}{2}$ the diagonal of the square.

Equations (4) and (5) give a calculated inductance within 2% of the measured value, which is considered to be excellent agreement.

For example:

For 4' x 4' antenna with 20 turns

ℓ = 2.75 inches N = 20

a = 1.19 x 24 = 28.92 inches

Calculated L = 1.45 mh Measured L = 1.42 mh

and for 3' x 3' antenna with 5 turns

ℓ = 2.0 inches

a = 1.19 x 18 = 21.42

Calculated L = 68.7 µh Measured L = 70 µh

EFFECT OF RESISTIVE LOADING ON ANTENNA VOLTAGE OUTPUT

The antenna as a source of voltage for a receiver has an internal impedance. If the receiver input impedance is very low (which it may be in the case of a simple transistor input stage) then the input impedance of the receiver can load down and reduce the antenna output voltage to a very small value. In addition, the Q of the tuned antenna circuit is reduced, further reducing the antenna output signal. For these reasons it is useful to have some idea of what the effective tuned antenna impedance is. Fig. 3.0-4, a and b, shows the effect of resistive loading on the relative signal output for two different antennas. As can be seen from loading to $\frac{1}{2}$ open-circuit value the impedance of the large 20 turn coil is approximately 5000 ohms, and of the smaller 5 turn coil

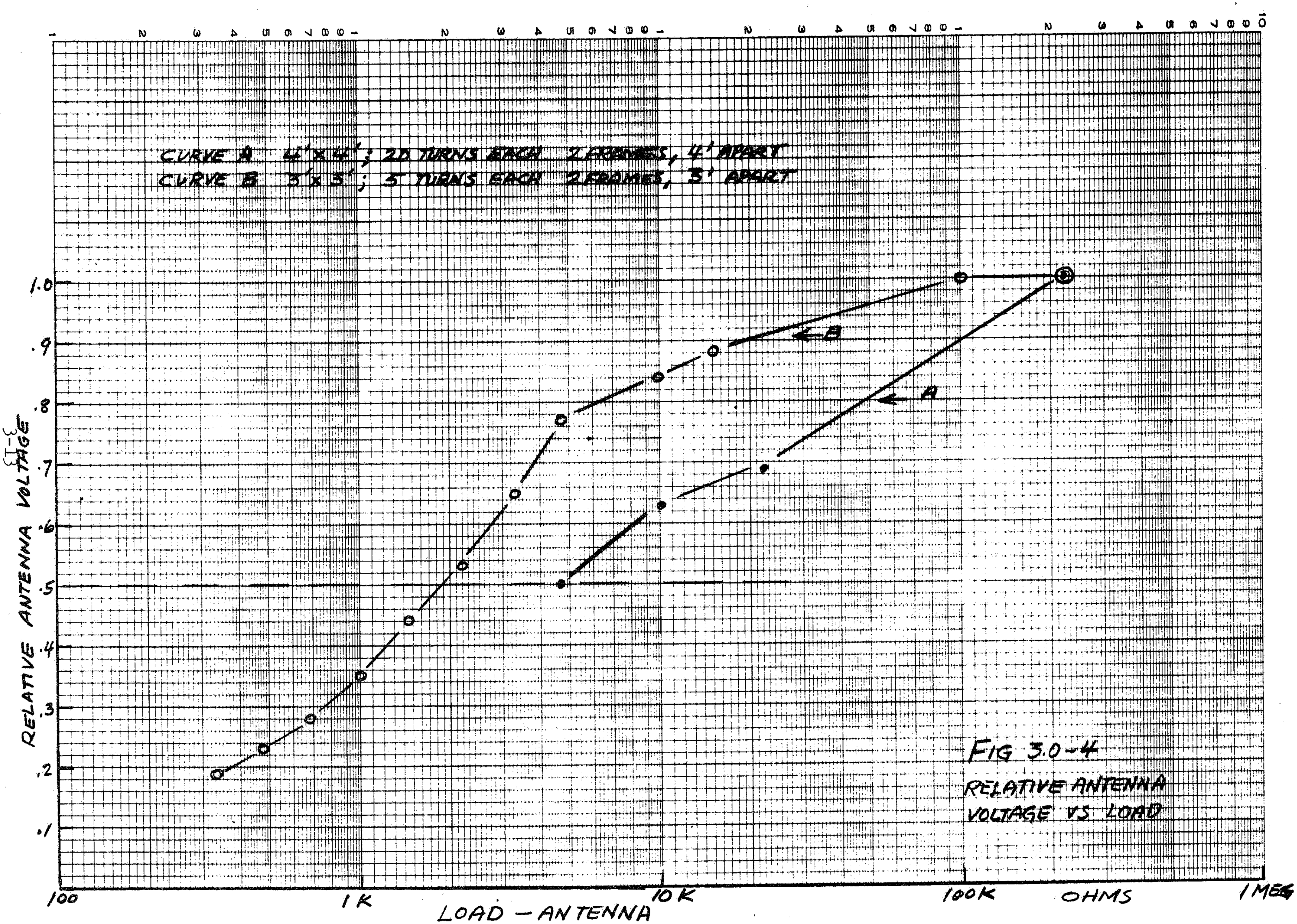

FIG 3.0-4
RELATIVE ANTENNA VOLTAGE VS LOAD

is about 2000 ohms. This is sufficiently low that a receiver input impedance in 10 K to 20 Kohm range or higher will not significantly reduce the signal from antennas of this order of dimensions.

ANTENNA MEASUREMENTS

Signal strengths for various antenna configurations were measured. The coordinates of measurements are defined in Fig. 3.0-5.

Measurements were made in the region of the first quadrant of the X-Y plane and in the first quadrant of the Z-Y plane out to $Z = S/2$, where S is the separation of the two antenna frames. In the cases where the frames were spaced so that $S < D$, measurements were made in the second quadrant of the Z-Y plane. Because of symmetry this covers completely the whole region inside the antenna coils and extends to the region of interest for cages enclosed by the frames. Not all measurements made are plotted in the graphs of signal strength as the signals are continuous and would lead to confusion. Curves are shown for the selected lines A, C, D, as shown in the figure. These lines are at:

A - the center of the antenna coil

C - at 2/3 of the diagonal from center to the corner

D - at the inside edge of the antenna coil

Coordinates of line A (Z = 0, Y = 0, Z = Z)

C (X = 8", Y = 8", Z = Z)

D (X = 12", Y = 12", Z = Z)

24" x 24" 10 turns tuned C = .0006 μfd

¼" spacing No. 15 wire load R = 10K

Single frame

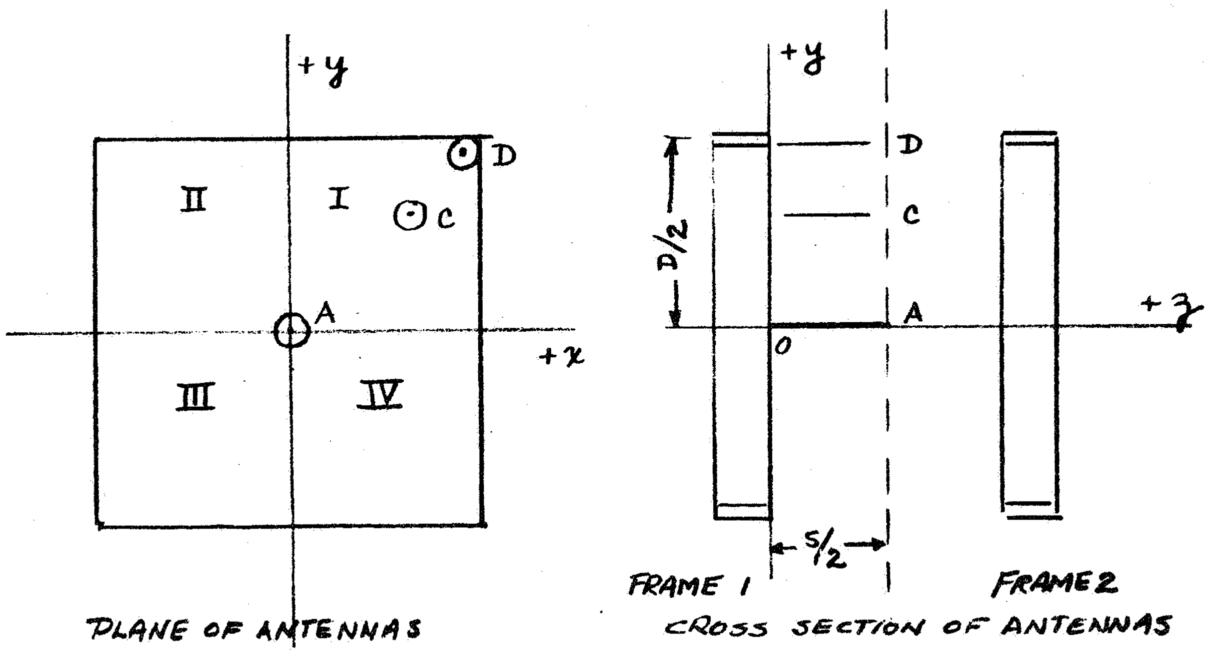

FIG 3.0-5 COORDINATES FOR SIGNAL MEASURMENTS

SIGNAL PEAK TO PEAK

A				C				D			
X (in)	Y (in)	Z (in)	Signal mv	X (in)	Y (in)	Z (in)	Signal mv	X (in)	Y (in)	Z (in)	Signal mv
0	0	0	17	8	8	0	28	12	12	0	30
		4	14.5			4	11.5			4	3.0
		8	10.0			8	6.0			8	2.0
		12	6.5			12	4.1			12	1.5

Same as above but 2 frames 2 feet apart, tuning capacity C = .0002; R_L = 10K

X = Y = 0		X = Y = 8		X = Y = 12	
3	Signal	3	Signal	3	Signal
0	14.5	0	22.5	0	28
4	12.5	4	11.5	4	3.0
8	10.0	8	6.3	8	3.0
12	8.8	12	6.0	12	2.0

Same as above 2 x 2 ($\frac{1}{4}$" spacing) 10 turns each

Spacing of antennas 12" (inside of frame to inside of frame)

A) X = Y = 0		C) X = Y = 8		D) X = Y = 12	
Z (in)	Signal (mv)	Z (in)	Signal (mv)	Z (in)	Signal (mv)
-6	7.5	-6	7.5	-6	2.5
0	10.0	0	13.8	0	14.5
6	9.5	6	7.0	6	2.8

3' x 3' antennas

2 frames

5 turns each No. 25 wire $\frac{1}{2}$ spacing

C = .001

R_L = 10K

Frame spacing S = 3' (36 inches)

Signal peak to peak

A) X = Y = 0

Z (in)	Signal (mv)
0	5.0
6	4.5
12	3.8
18	3.2

C) X = Y = 12

Z (in)	Signal (mv)
0	9.0
6	4.0
12	2.5
18	2.0

D) X = Y = 18

Z (in)	Signal (mv)
0	13.5
6	1.5
12	1.0
18	< 1.0

Same as above but frames spaced 18" to inside edge

A) X = Y = 0

Z (in)	Signal (mv)
-9	4.8
0	6.5
9	6.5

C) X = Y = 12

Z (in)	Signal (mv)
-9	4.1
0	9.5
9	5.0

D) X = Y = 18

Z (in)	Signal (mv)
-9	2.0
0	14.0
9	1.0

4' x 4' antennas

2 frames

20 turns each

No. 25 wire, spaced 1/8"

c = < 0 (i.e., could not add capacity to tune)

R_L = 10K (corrected to this value)

Frame spacing S = 48"

Signal peak to peak

Telemeter - high power breadboard signals corrected to Mark IV equivalent

A) X = Y = 0

Z (in)	Signal (mv)
0	3.8
12	3.6
24	2.4

C) X = Y = 16

Z (in)	Signal (mv)
0	6.3
12	2.7
24	1.9

D) X = Y = 24

Z (in)	Signal (mv)
0	12.8
12	1.7
24	1.2

These measurements (4' x 4') can only be compared with the 2 foot and 3 foot frames with caution as they were made with no loading and with a high power telemeter putting out a signal estimated at about 3 times that of a Mark IV telemeter and of a higher repetition rate. The signal levels shown are corrected for both loading and telemeter signal to be equivalent to Mark IV generator and with a 10 kilohm loading.

ANTENNA MODIFICATIONS

In the course of investigating the antennas described in the previous section, several other antenna configurations and circuit arrangements were tried in an effort to improve the signal and/or reduce the noise. It was noted that a transistor radio placed inside of one of a pair of connected antennas received a signal of appreciable magnitude when the telemeter was placed inside the other antenna of the pair. A logical extension of this configuration was to use a large antenna as the signal pickup antenna with a small antenna wrapped around the transistor radio, Fig. 3.0-6. This coupling was further improved by wrapping the second small antenna directly on the ferrite loop antenna of the radio. The chief advantage of this arrangement was that very few (in fact, one) turns of the primary receiving antenna were sufficient to give a strong signal from the radio, the radio acting as a high gain tuned amplifier loop coupled to the telemeter receiving antenna. A cursory investigation of this configuration was carried out.

While it is difficult to report quantitative results for this arrangement, the following was determined for the configuration shown.

A. More than a single turn on each loop did not improve signal or signal-to-noise ratio appreciably.

B. Five to ten turns on the ferrite loop saturated the radio amplifiers.

C. Tuning of the loop linkage improved the signal considerably (radio previously tuned to telemeter carrier).

D. The spacing shown gave the maximum volume with usable signal.

E. The volume with usable signal is considerably less than the 4' x 4' x 4' volume "enclosed" by the antennas. This was estimated to be about $2\frac{1}{2}$' x $2\frac{1}{2}$' x $2\frac{1}{2}$'.

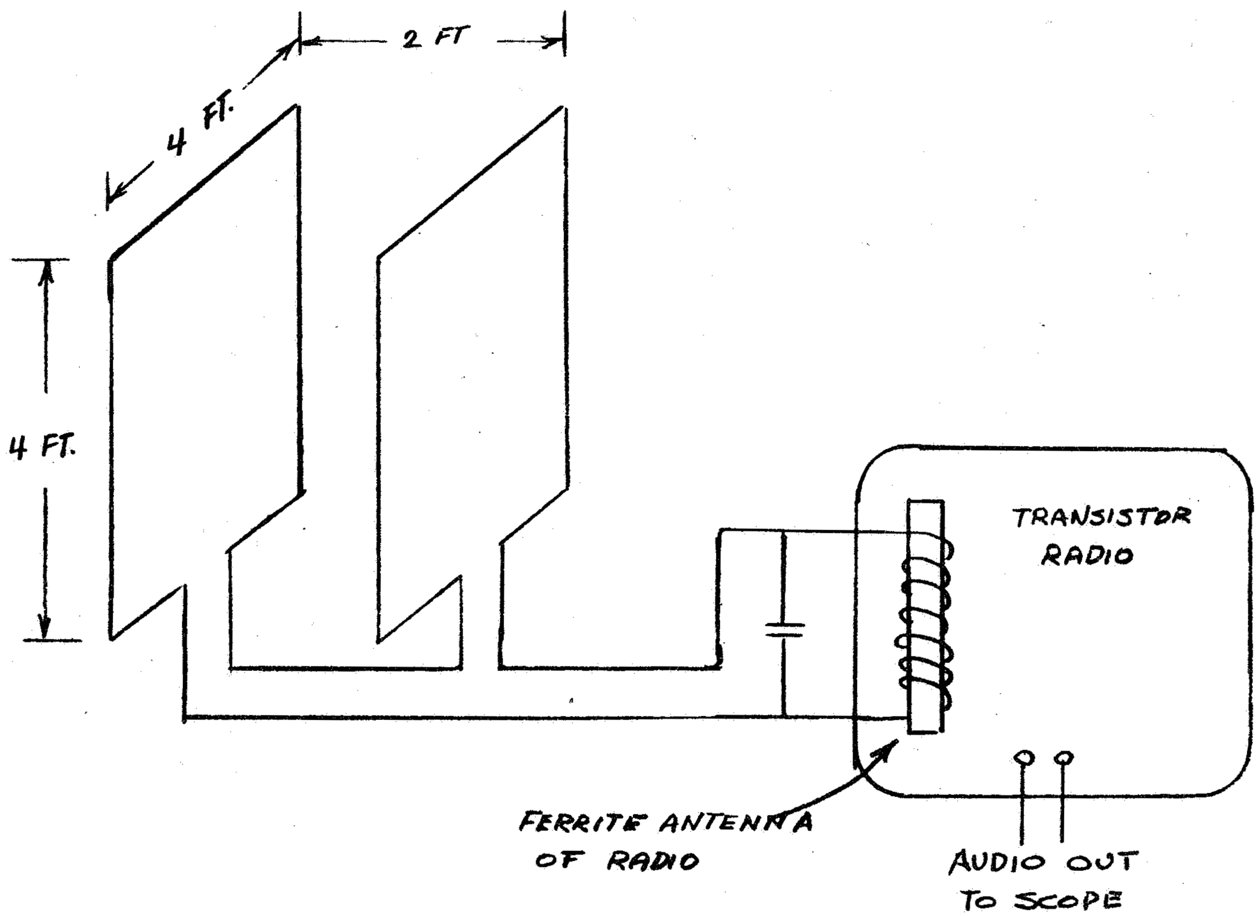

FIG 3.0-6 ANTENNA COUPLED TO TRANSISTOR RADIO.

F. The usable volume depended primarily on the noise (pulses at 60 and 120 cps) picked up by the antenna configuration. At this locality during daily working hours the noise was particularly strong.

At this time, this configuration is still considered promising but has not yet been developed to a point where it will replace the smaller standard multiloop antenna pairs operating into a standard amplifier. The advantages of this system are twofold: one, that inexpensive high gain tuned amplifiers (miniature transistor radios) could be used in place of custom designed standard amplifiers; and two, that a single turn pair of antennas is, from a practical point of view, very easy to construct, maintain and operate around an animal cage. Two single turns of wire are especially easy to disassemble to obtain access to an animal cage.

3.1 REFERENCES

3-1 Gibson, R. J., Goodman, R. M., and Marmarou, A., "Instrumentation for the Study of Biological Rhythms," Section 5.2-1, Vol. 1, F-B2029, October 1962 - November 1964, NASA Contract No. NASr-146

3-2 Slater, L. E., (editor) Biotelemetry, Pergamon Press, McMillan Company, 1963.

3-3 Greene, F. M., "The Near-Zone Magnetic Field of A Small Circular Loop Antenna," Journal of Res. Sec. C, Eng. and Instr. Vol. 71C, October - December 1967, pp 319-326.

3-4 Harrington, R. F., and Mautz, J., Inst. of Elec. Engrs. Proceedings Vol. 115, January 1968, pp 68-76.

3-5 Gibson, R. J., Goodman, R. M. and Marmarou, A., "Instrumentation for Biological Research," Final Report F-B2299, Nov. 1964 - March 1966, NASA Contract NSR-39-005-018.

3-6 Radiation Designer's Handbook, F. Langford Smith (editor) 4th Ed. 1952, RCA.

4.0 CALIBRATION CURVES OF MARK IV TELEMETERS

The temperature vs. pulse count from a typical temperature telemeter (No. 404 Mark IV) can be rather accurately approximated by a quadratic equation.

This telemeter had the calibration as shown in Fig. 4.0-1. The PRF was measured to the nearest unit and the temperature to the nearest one tenth degree Celcius. A smooth curve was drawn through the five points shown. From this curve a table of temperature PRF pairs was prepared at one-half degree intervals. The first, second, and third differences of PRF were obtained. The second difference was constant to plus or minus one unit of PRF from 29.5 to 41.5°C using the extrapolated smooth curve values. This would indicate that a second degree of quadratic curve should give an excellent fit. Using the PRF values at each 2° (30, 32, etc.) a least square fit equation was obtained.

The normal equations for a least squares second degree equation are as follows:

T = temperature °C N = number of observations

P = PRF

$$ET = Na + bEP + CEP^2$$

$$EPT = aEP + bEP^2 + CEP^3$$

$$EP^2T = aEP^2 + bEP^3 + cEP^4$$

Coded values of P and T were used to reduce mass of arithmetic yielding an equation of the form.

TELEMETER NO. 404

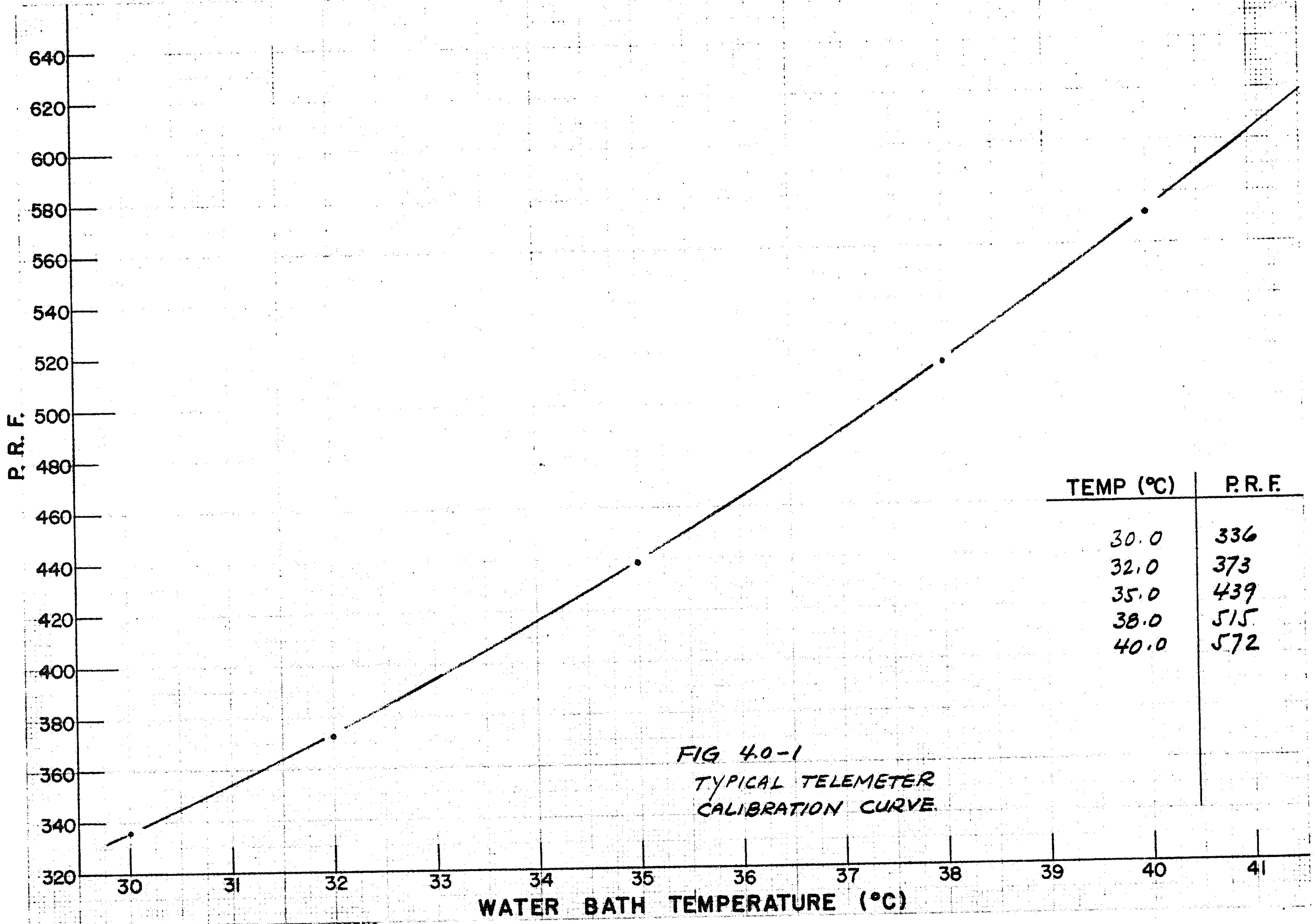

TEMP (°C)	P.R.F.
30.0	336
32.0	373
35.0	439
38.0	515
40.0	572

FIG 40-1
TYPICAL TELEMETER CALIBRATION CURVE

FIRL, BIOINSTRUMENTATION – MK IV SYSTEMS

$$T = a + bP \times cP^2$$

Using six points from the curve the following least squares quadratic equation is obtained.

$$T = 7.291 + .0821\ P - 44.8785 \times 10^{-6}\ P^2$$

or

$$T = 7.291 + \frac{P}{12.075} - \frac{P^2}{22.282.405}$$

or, in the most convenient form for calculation

$$T = 7.291 + \left(\frac{P}{12.076}\right) - \left(\frac{P}{149.273}\right)^2$$

From this equation, knowing a value of P we may calculate a value of T. To test its accuracy we give some typical values.

P	T(meas.)°C	T(Calc.)°C
336	30.0	30.048
439	35.0	34.995
572	40.0	39.974

As can be seen these values check to within 1/20°C, which is approximately one count. No better correspondence can be expected.

Several other telemeters will be checked in the same way, and if a quadratic curve fits them as well as it fit this one, a program will be written so that the computations may be done on a computer for each telemeter as it is calibrated. The formula will then be included with each calibration curve. These calculations are quite time consuming on a desk calculator and without a computer programmed to handle them it is impractical to process more than a few units.

5.0 CONTINUED MULTICHANNEL IMPLANTABLE TELEMETER DEVELOPMENT

As the effort began this period, it became apparent to us that the evolution of a "generally applicable" subcarrier oscillator (SCO) design would be a desirable achievement.

Thus, we defined our initial design problem:

> Design a subcarrier oscillator with a high input impedance, a minimum power consumption, the capability for direct or ac drive, and acceptable stability over the biological temperature range.

To this end, we studied three attractive solution approaches in sequence. Early results of the first approach were reported at the Stockholm meetings (5-1).

5.1 THE COMPLEMENTARY MULTIVIBRATOR SCO

This development was reported in some detail in our last annual report (5-2). It was amply clear from considerations of cross-channel interference that the use of pulsatile modulation could cause undesirable difficulties, particularly as the number of transmitted parameters increased and the SCO center frequencies drew more closely together.

Of equal pertinence was the fact that while such modulators required only 4 or 5 x 10^{-6} amperes of current for operation, they proved difficult to control with high frequency data content and evidenced some instability when so controlled. As we proceeded to improve stabilization and sensitivity the circuit requirements grew more complex, and the current requirements grew past our ten microampere target.

Our conclusions with regard to the complementary multivibrator type of SCO were as follows:

a. Desirable sensitivity was not available without substantially exceeding the 10^{-5} ampere level.

b. SCO stability was a matter of concern.

c. Circuit complexity was growing seriously

d. Circuit output was not sinusoidal, a matter of consequence at the receiving end of the system.

Figure 5.1-1 illustrates the basic complementary multivibrator SCO. This circuit is valuable as an extremely simple and sensitive, thermistor-controlled, temperature sensing SCO.

5.2 THE SQUEGGING SCO

The old Mark IV implant development (5-3, 5-4) based on the squegging or blocking oscillator, appeared to offer some promise of useful application. Such circuits were operated at current levels as low as 2.5×10^{-6} amperes.

The functional approach to the design is illustrated in Fig. 5.2-1. The basic design is premised on the fact that the SCO squegging rate is controlled by the discharge time constant associated with capacitor C.

It appeared therefore that an extremely simple SCO could be designed for great sensitivity, high input impedance and general utility. Typical developmental circuits are illustrated in Fig. 5.2-2. It will be noted that the circuits are extremely simple. Also note that

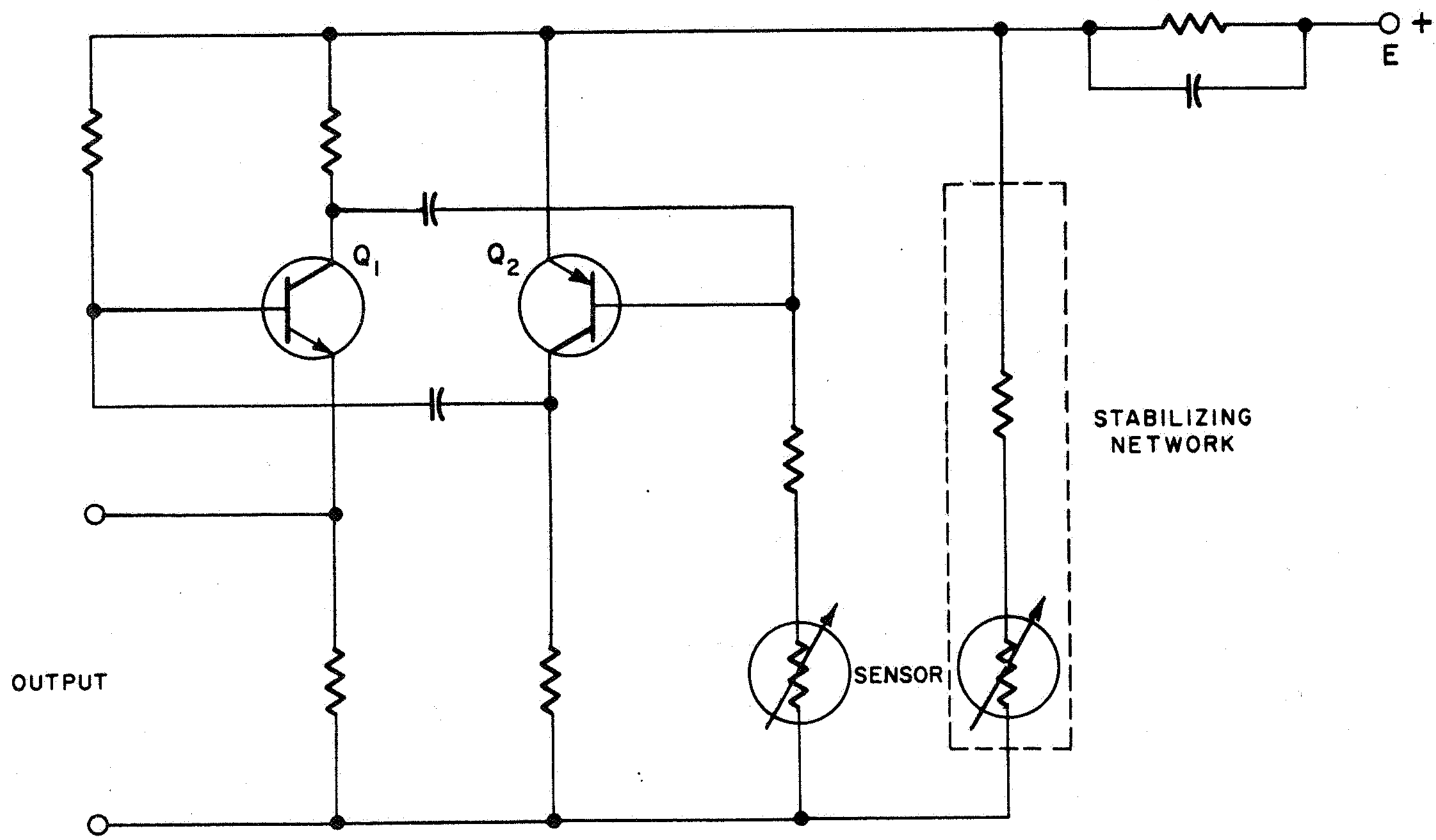

Fig. 5.1-1 Circuit, Complementary Multivibrator SCO

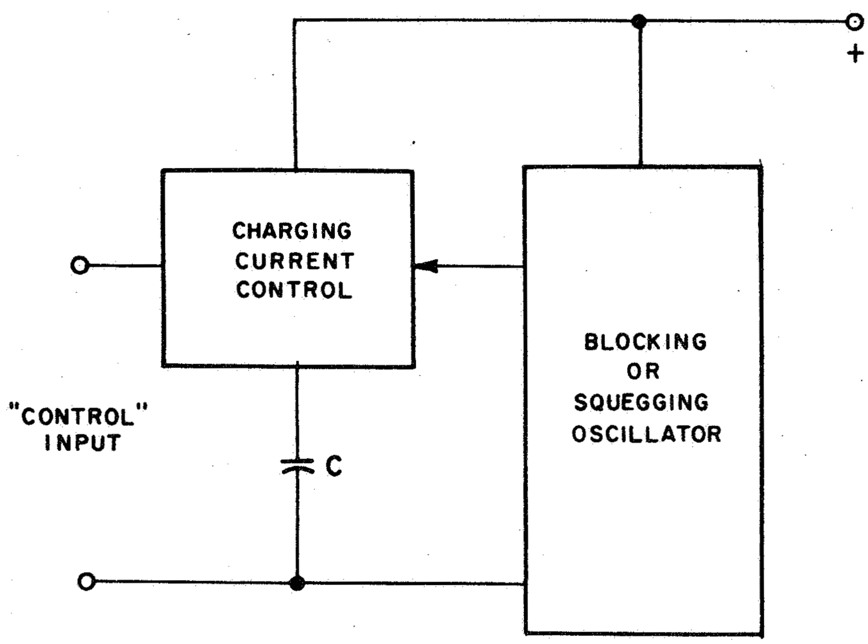

Fig. 5.2-1 Functional Diagram, Squegging SCO

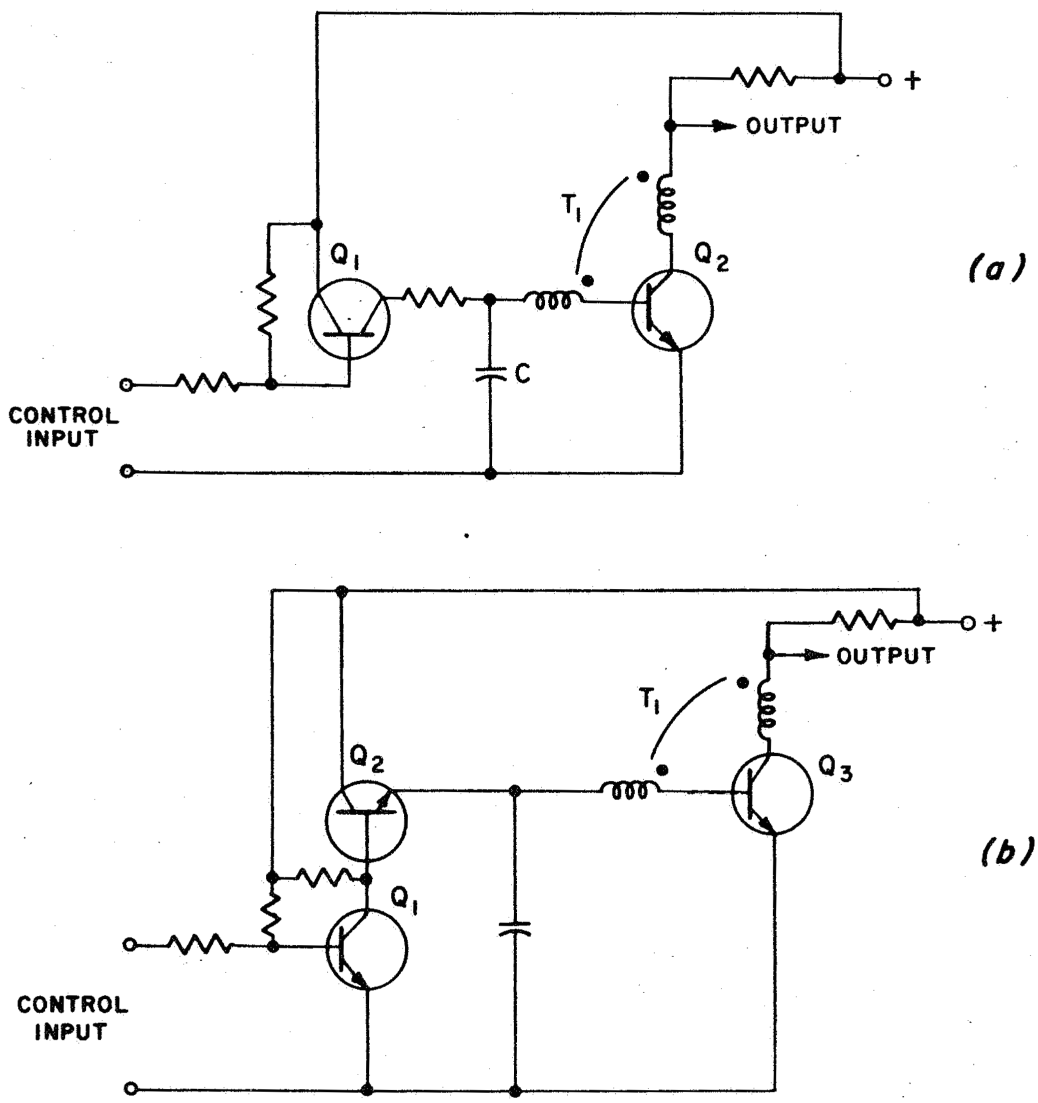

Fig. 5.2-2 Circuit, Experimental Squegging SCO

transformer T_1 is an essential component in the circuit design.

As a practical matter, transformer T_1 must be extremely small and light in weight since several units are to be required in the complete telemeter. Further, no inductive coupling can be permitted between transformers of the various SCO channels. External magnetic fields generated by these transformers can be minimized by the use of toroids as winding cores. Fig. 5.2-3 is a photograph of a typical experimental transformer used in the circuit design.

The size of the transformer is quite acceptable. Its weight is ca. 0.02 grams.

The magnetic core has the following characteristics:

Material:	Indiana General, 0-6
Internal Diameter:	0.050 inches
Outside Diameter:	0.080 inches
Magnetic path length:	0.204 inches
Permeability (μo):	about 3000

The wire used in the windings is No. 44 Formvar.

Typical current requirement for the circuits of Fig. 5.2-2 is $9 - 11 \times 10^{-6}$ amperes. The circuit proved to have serious disadvantages in spite of its apparent simplicity.

a. The transformer T_1 core was, of necessity, selected from high permeability material. This represented the only means available to evolve a transformer with sufficient winding inductance to produce output pulse widths useful for our purposes. However, such high permeability core materials have poor temperature stability. Any tradeoff to obtain core stability would result in unacceptable

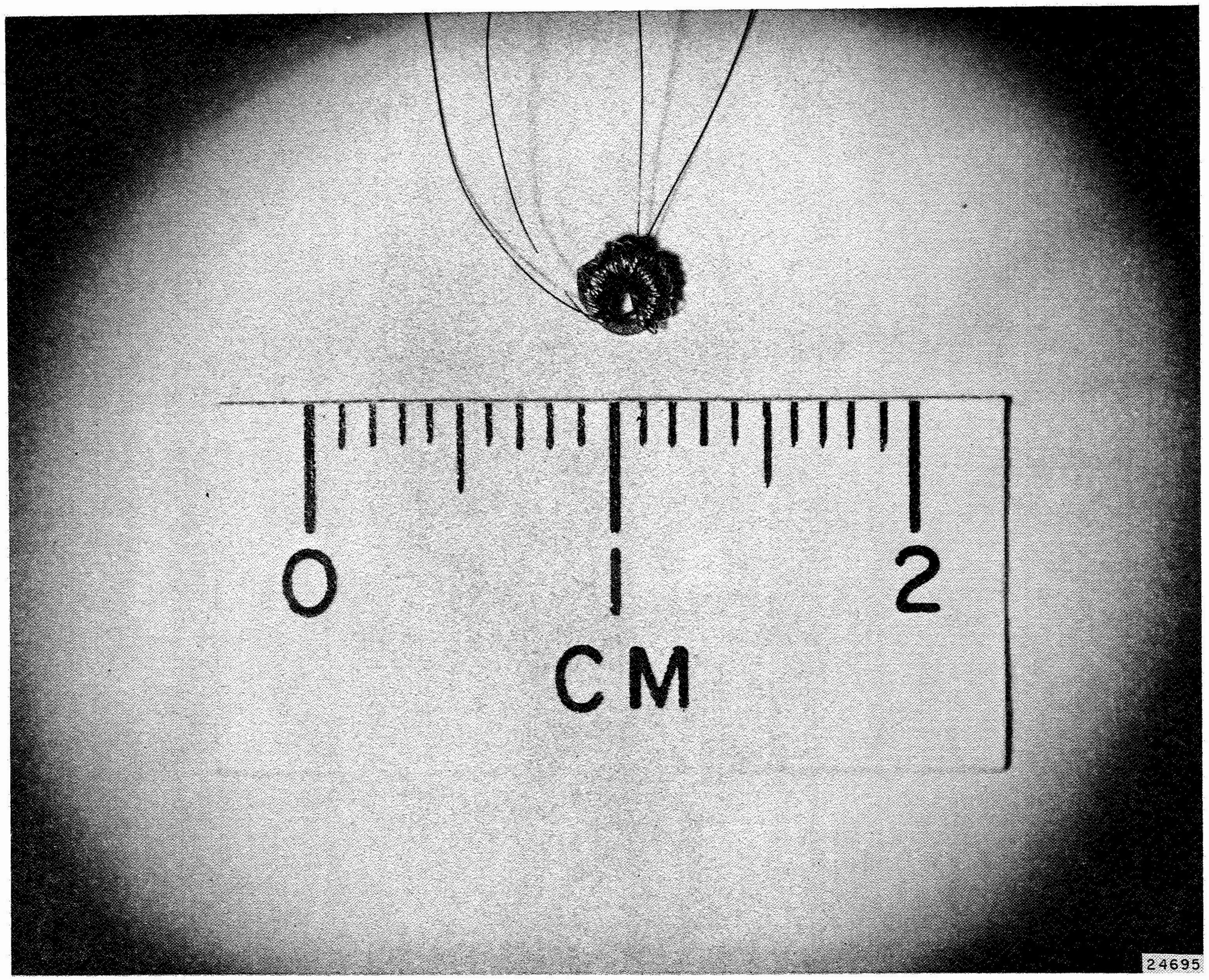

Fig. 5.2-3 Squegging SCO Transformer

increases in core size and weight and winding size.

b. The circuit was sensitive to firing-point jitter, a matter of particular importance at the relatively low power levels involved. This meant that such SCO's would be quite susceptible to extraneous electrical noise sources.

c. Output from SCO was not sinusoidal

5.3 THE SINE WAVE SCO

Based on our experiences described above we decided that a major effort was worthwhile to evolve a micropower SCO with sinusoidal output. It should be clear that tacit in this decision is the statement that an effort to convert the pulsatile outputs of the previously described SCO's is not considered expedient. This is based on the fact that necessary filter networks would have to be active and would be costly in power and complexity.

We then examined the phase-shift and Wien-Bridge oscillators as potentially useful. Because of voltage source limitations we selected the Wien-Bridge circuit configuration.

The basic oscillator is shown in generalized form in Fig. 5.3-1. Fig. 5.3-2 illustrates a typical experimental oscillator circuit. Oscillators of the type illustrated in Fig. 5.3-2 were constructed and operated at approximately the following IRIG modulation frequencies.

Freq. (Kc/s)	Current Drain
1.3	7×10^{-6} amperes
1.7	"
2.3	"
3.9	"

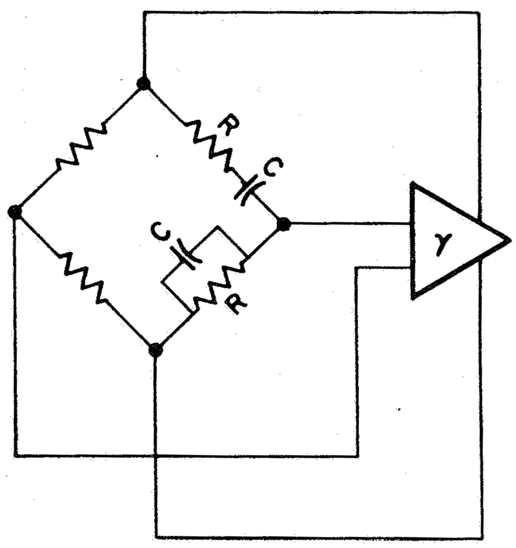

Fig. 5.3-1 Wien Bridge Oscillator, Generalized Form

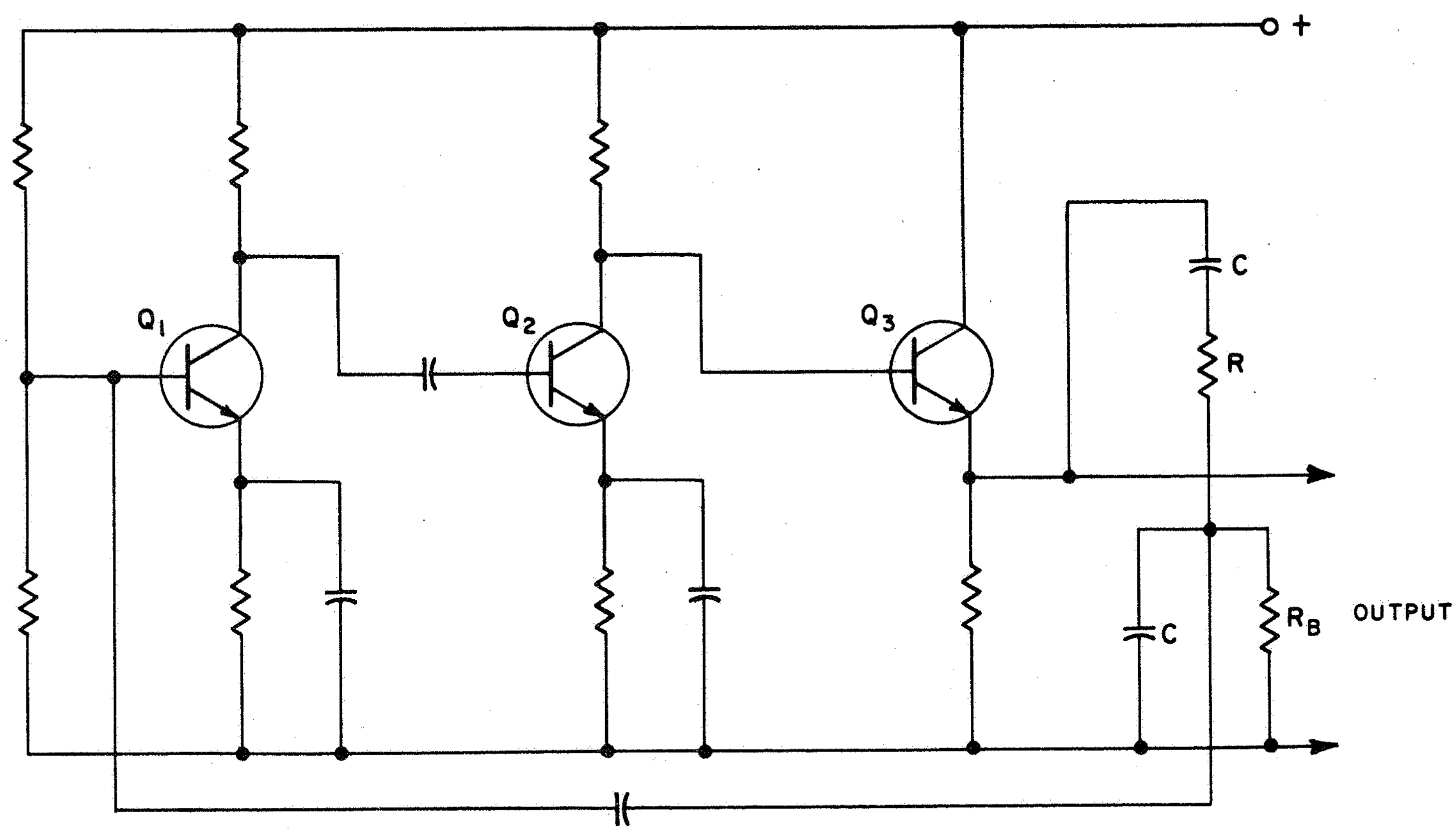

Fig. 5.3-2 Experimental Circuit Oscillator

Freq. (Kc/s)	Current Drain
5.4	7×10^{-6} amperes
7.35	"
10.5	"

The current requirement was very promising, and circuit stability appeared reasonable. In order to determine the kind of variation in one leg of the bridge (R_B in Fig. 5.3-2) required for a frequency deviation, we varied R_B empirically and resultant data appears in curves Figs. 5.3-3, -4, -5, -6 and -7. Theoretical oscillator frequency may be expressed as

$$f_o = \frac{1}{2\pi(R_1 R_2 C_1 C_2)^{\frac{1}{2}}}$$

and, of course, for $R_2 = R_B$, a theoretical resistance variation for a given f_o variation can be calculated. Unfortunately, exact values for R_1 and R_2 in the circuit are not available so that differences from nominal as large as ± 10% were possible, and as much as ± 20% between R_1 and R_2 is possible. Therefore, reference, for example, to Fig. 5.3-7 shows $R_B \approx 86K\Omega$ at $f_o = 10.5 \times 10^3$ and a $\Delta R_B = 68K\Omega$. Calculation of ΔR for a 15% shift in f_o can be expressed as

$$\Delta R = \frac{1}{R} \left(\frac{.1871}{f_o C}\right)^2 - R$$

where ΔR is in correspondence to $f = .85\ f_o$.

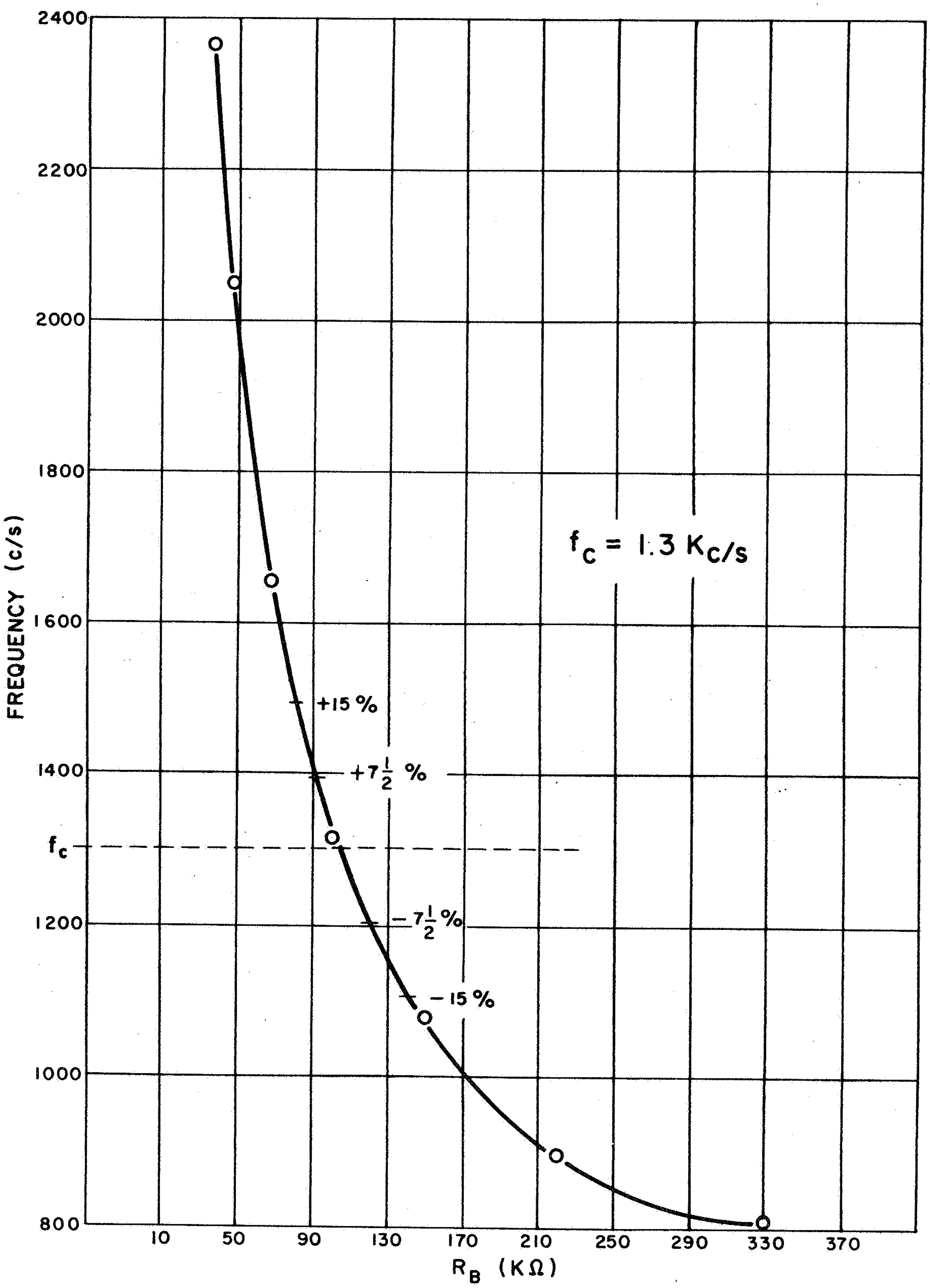

Fig. 5.3-3 Curve, R_B vs f, 1.3 Kc/S Channel

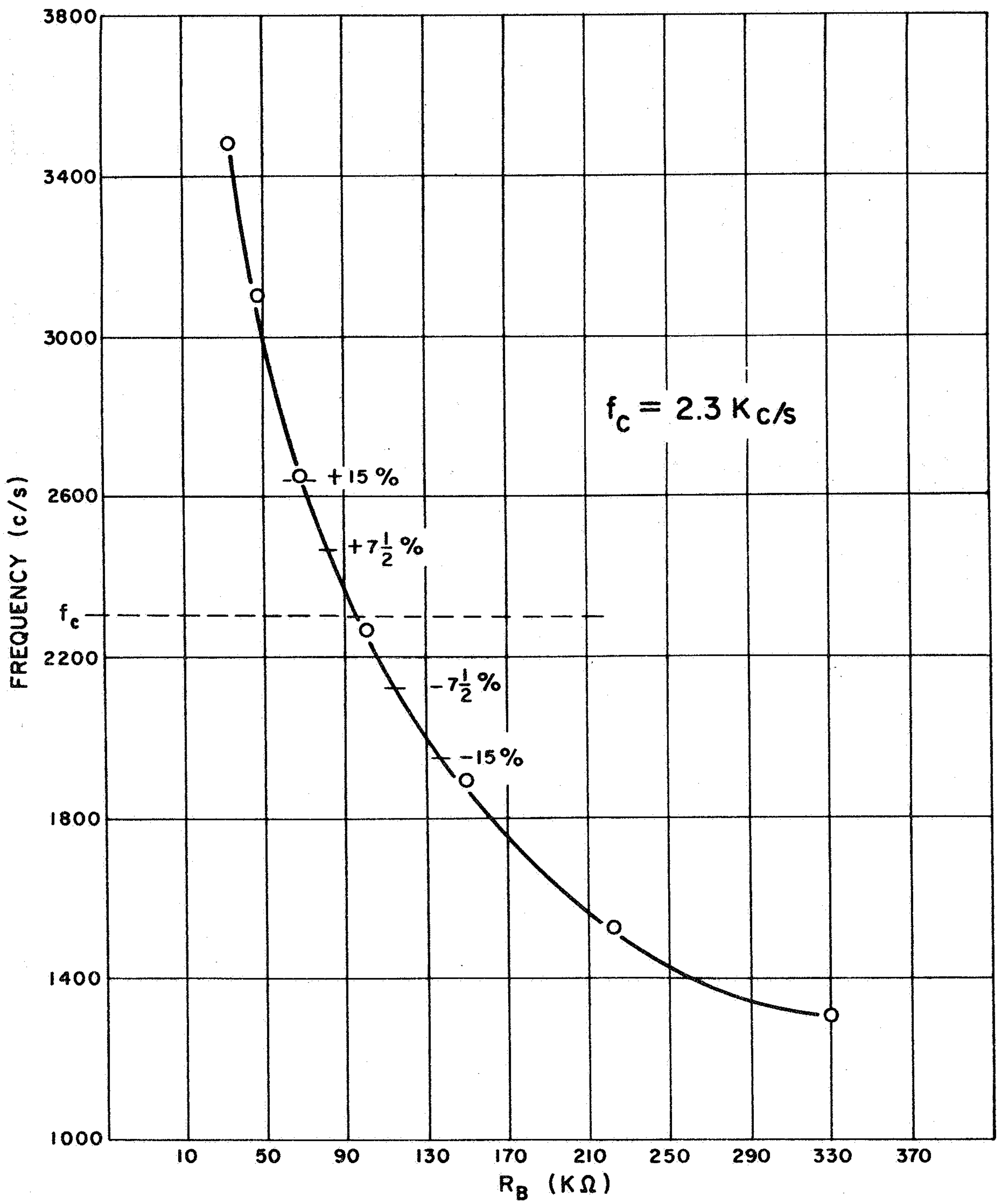

Fig. 5.3-4 Curve, R_B vs f, 2.3 Kc/S Channel

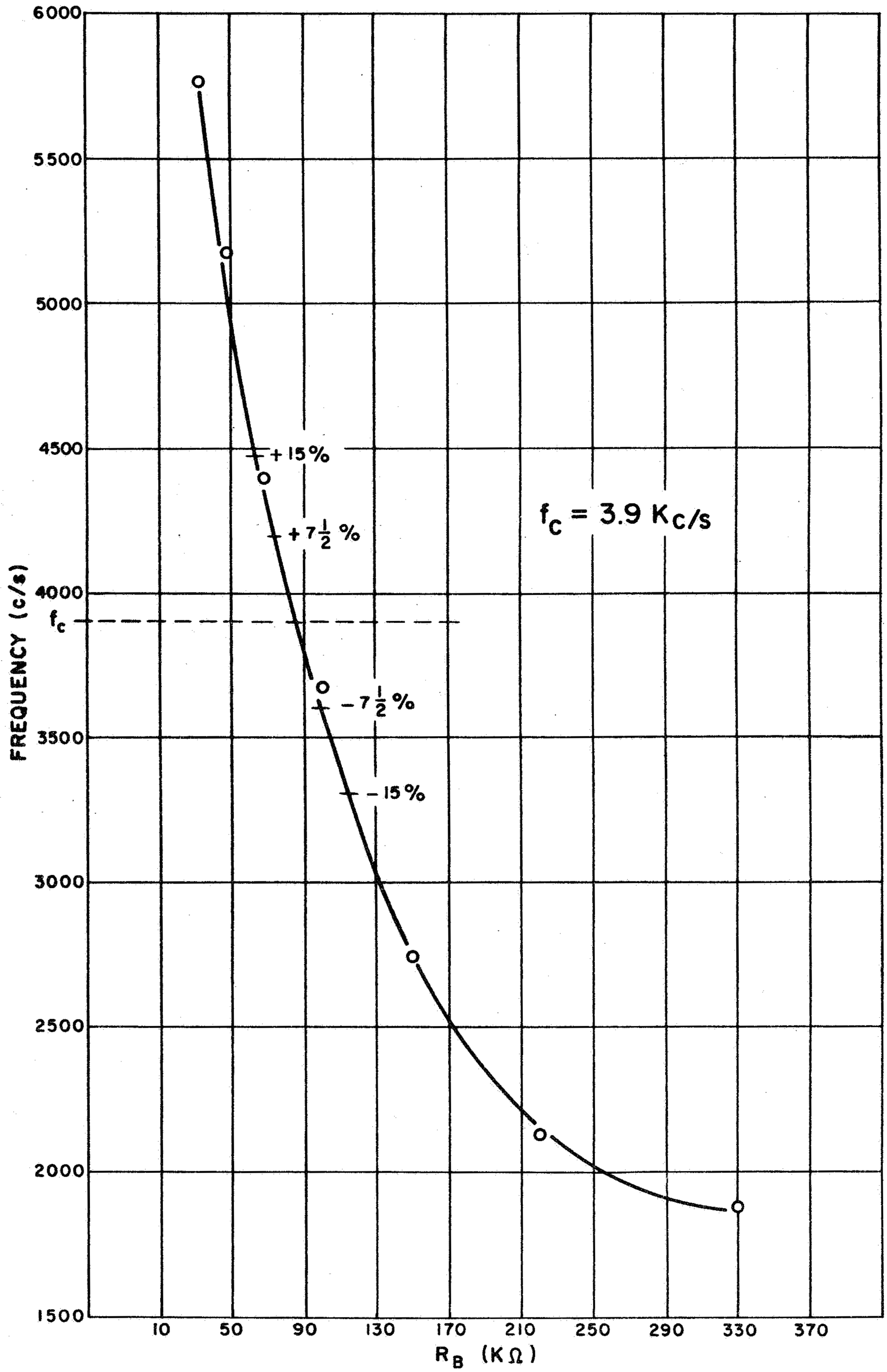

Fig. 5.3-5 Curve, R_B vs f, 3.9 Kc/S Channel

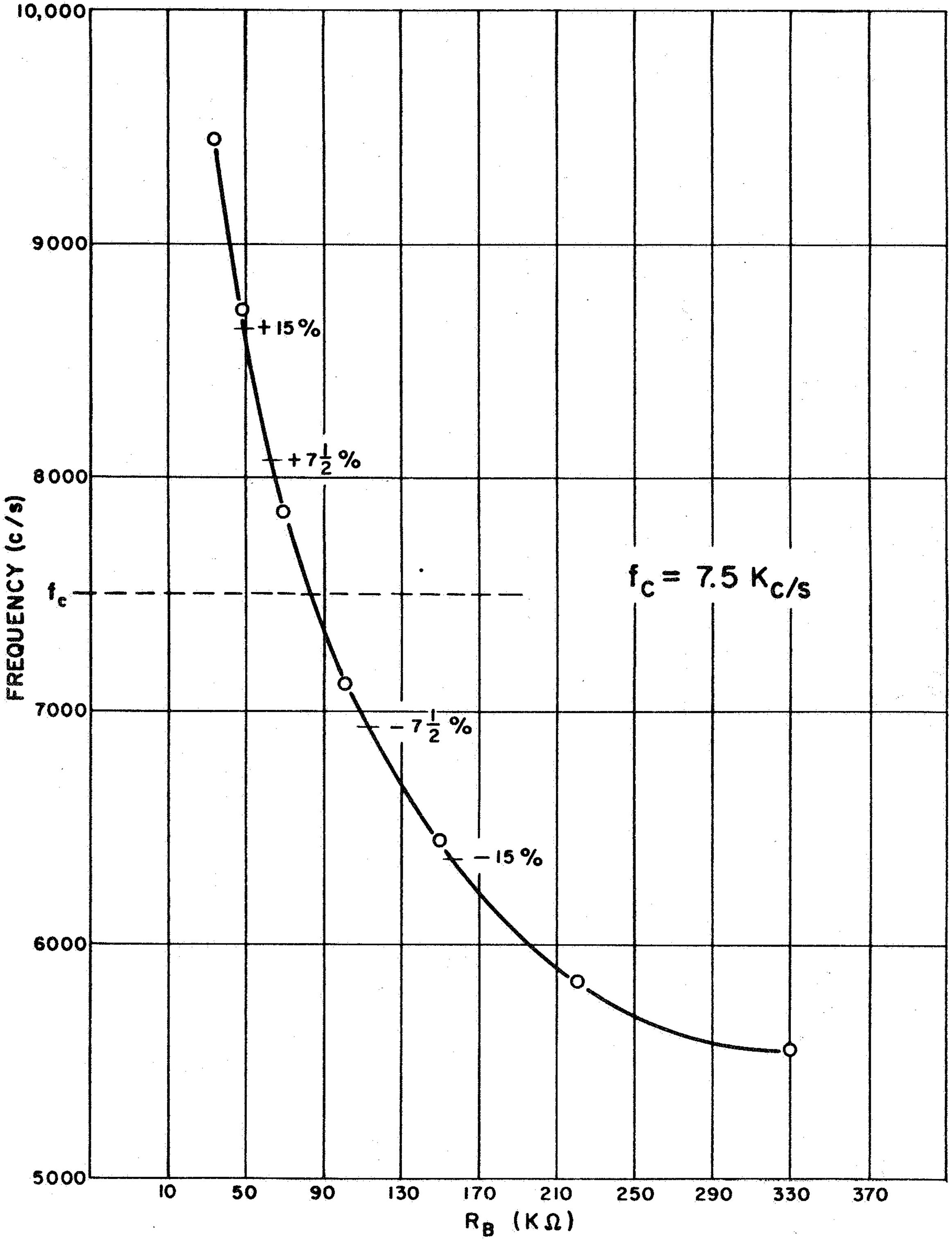

Fig. 5.3-6 Curve, R_B vs f, 7.5 Kc/S Channel

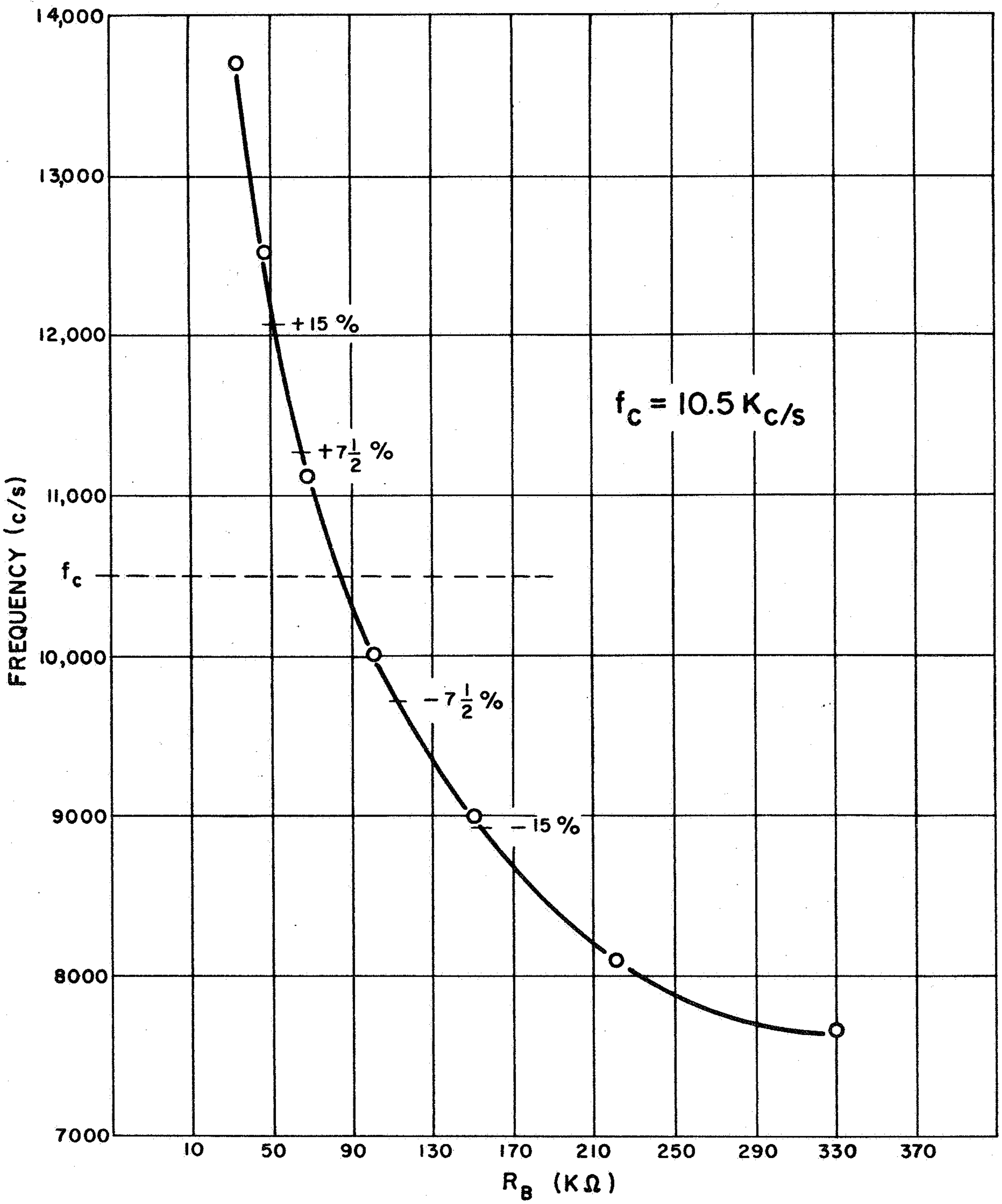

Fig. 5.3-7 Curve, R_B vs f, 10.5 Kc/S Channel

Based on the use of the following nominal data:

$$R_1 = R_2 = 10^5 \text{ ohms}$$

$$C_1 = C_2 = 1.51 \times 10^{-10} \text{ f}$$

$$\Delta R = 39 \times 10^3 \text{ ohms}$$

Of course, the important aspect here was the order of magnitude of resistance shift required. The portent of these measurements and theoretical calculation was that sensitive control should be possible and that we might run into a serious temperature stabilization problem.

The simple circuit of Fig. 5.3-2 was used as a temperature controlled SCO by replacing R_B in part with a thermistor. Operation was excellent.

Our first efforts for more sophisticated modulation control utilized fairly standard transistors. However, it became quite clear that substantial input impedances could not be expected in return for the simplicity and low levels of bus voltage at which we wished to operate. For example, the transistor TIS22 could not be expected to provide (even taking an optimistic view) an input impedance in excess of 1.6×10^6 ohms, given

$$h_{oe} \approx 40 \times 10^{-6}$$
$$h_{fe} \approx 60$$
$$h_{re} \approx 8 \times 10^{-4}$$
$$h_{ie} \approx 1.5 - 11 \times 10^3 \Omega$$

then

$$r_b = 250$$

$$r_c = 1.55 \times 10^6$$

$$r_e = 20$$

$$\alpha = .984$$

and

$r_c \approx 1.6$ megohms for the common collector configuration

An effort was made to trade impedance for gain, but it was costly in complexity and from the viewpoint of circuit stabilization. Stimulated by our conversations with Mr. Cliveden Weller of the Holly Hill Laboratory in London (See Section 8.0), we resolved to apply the field effect transistor. The first circuit studied is illustrated in Fig. 5.3-8. The input impedance for this SCO is limited primarily by the Gate bleeder chain (R_1, R_2) as indicated. This can be circumvented if desirable, in specific applications. The simple circuit used has an input impedance > 3×10^6 ohms and produces about 2% modulation to the channel frequency for about 1.6×10^{-3} volts input. The performance of the basic circuit is expected to improve markedly with the receipt of other type FET's for which procurement has been initiated. The total current requirement for the illustrated SCO is 7×10^{-6} amperes.

Because of our immediate interest in SCO sensitivities on the order of 100 μv or less, we proceeded to variations of the circuit of Fig. 5.3-8. To date, sensitivities on the order of 2% for 100 μv peak to peak signal input have been attained. Maximum current drain has not exceeded 10 μa amperes. As noted above, receipt of additional transistor types will further improve performance.

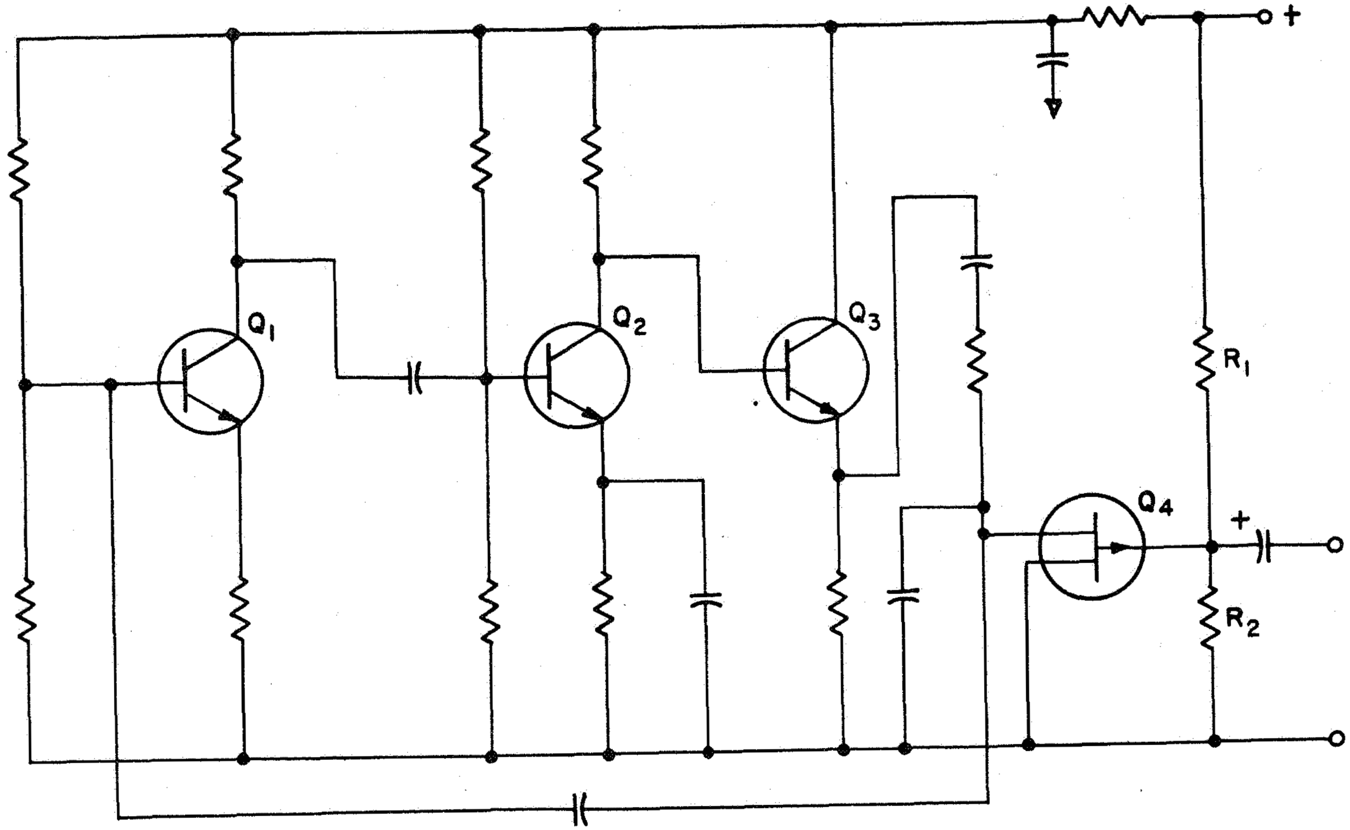

Fig. 5.3-8 Circuit, FET Controlled Wien-Bridge Oscillator

The problem of automatic circuit stabilization with ambient temperature variations was also attacked. To date, results are quite promising. Fig. 5.3-9 illustrates the performance of the SCO as a function of temperature with and without automatic compensation. Before discussing results in detail let us consider sources of SCO frequency variation with temperature.

Based on the frequency controlling components for Wien-Bridge oscillator operation,

$$f \propto \frac{1}{RC}$$

where $$R = \sqrt{R_1 R_2}$$

$$C = \sqrt{C_1 C_2}$$

Thus for a decrease in C, f rises and the same is true with R. The use of high dielectric constant capacitor chips in the circuit indicates that we can anticipate at least a 2% shift in f_o over the full biological temperature range. In addition, the pinch-off voltage at the critical FET (Q_4 in Fig. 5.3-8) will rise and thus reduce R_{DS} resulting in a frequency increase. A crude statement for this shift in pinch-off voltage is:

$$(V_P)_T = \pm \Delta C(2.2 \times 10^{-3}) + (V_P)_{25^oC}$$

Based on this equation and a knowledge of the FET bleeder chain values (R_1, R_2), it can be computed that R_1 must be reduced in value at the rate of approximately 38×10^3 ohms/^{o}C to offset the FET pinch-off voltage shift with rising temperature.

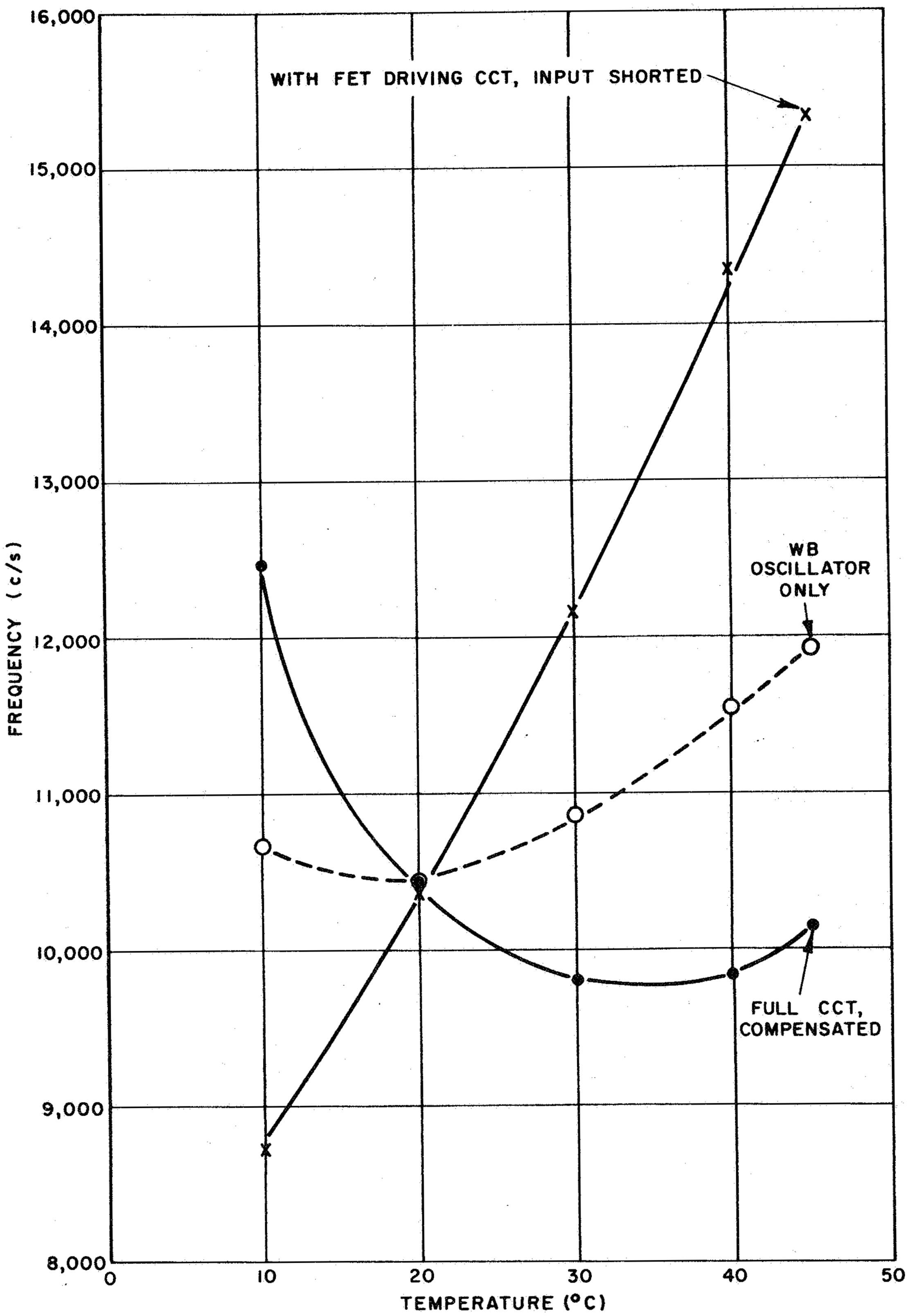

Fig. 5.3-9 Curves, SCO Performance vs. Temperature

Now referring to Fig. 5.3-9, we note for the Wien-Bridge oscillator circuit alone, that beyond 20°C a net rise in f_o occurs with temperature. In the range of 25 - 45°C this can be described as ± 7.1% and very much better in the range of 10 - 30°C. The full circuit including a three active element input circuit, has a characteristic response to temperature with a positive slope of about 170 cps/°C. Thus for the 20°C range discussed above we see at least a ± 16% variation in f_o over the indicated range.

Applying thermistor compensation in the control FET gate bleeder chain results in the third curve. In the range of 25 - 45°C this initial effort at compensation promises stability on the order of ± 2%. It also would appear from a study of the data that our first efforts may well represent overcompensation and that even further improvement may be attained.

Details of temperature compensation will be pursued further.

5.3.1 Future Plans

We believe we are now very close to attainment of the general purpose SCO originally described as desirable.

Because of the nature of the circuit, variable resistance sensors of high values are easily accepted as control elements; dc electrodes and high impedance voltage producing electrodes (such as pH electrodes) are acceptable, and ac voltage sources are acceptable.

Detailed data on the bandwidth for the ECG-SCO and temperature SCO will follow in an early report. However, no severe problems are anticipated for ECG in the frequency range from 0.05 cps to > 200 cps.

Temperature channel sensor time constants on the order of < 5 seconds are expected (after encapsulation).

Arrangements have been made to acquire implant experience with a first temperature-ECG unit, or temp -1, temp -2, temp -3, ECG unit as soon as it can be fabricated satisfactorily. The subject animal will be the rat or guinea pig.

5.4 THE TELEMETER OSCILLATOR

During the past year, a number of different tranistors were evaluated in the FM oscillator circuit. Results were as follows:

Transistor Type	Current Drain for Assured Operation (μa)
FSP-411/1	30+
D26G-1	30
LDA/406	30
T1XM101	40

In the coming period, certain of those listed units will be rechecked in a new physical circuit configuration. We also expect to process some new types.

A review of the circuit layout was made and future Mark V units will not carry the cell in the center of the tank coil. Oscillator current saving is anticipated as is a somewhat improved radiation efficiency. We expect these results because of reduced circuit losses and loading. We expect further, to make each oscillator easily adjustable in frequency over the 88-110 Mc/s range.

Cell location outside the tuned-circuit coil will permit its easier replacement and greater flexibility in the application of cells of various sizes.

5.5 REFERENCES

5-1. R. M. Goodman, "Simultaneous, Multi-Parameter Data from Implantable Telemeters," Digest of the 7th Internation Conference on Medical and Biological Engineering, Stockholm, Sweden, August 1967, 87.

5-2. R. J. Gibson, Jr., R. M. Goodman and I. R. Isquith, "Space Related Biological and Instrumentation Studies," FIRL Report A-B2299-1, March 1966 - March 1967, Section 4.4.

5-3. R. J. Gibson, Jr., R. M. Goodman, and A. Marmarou, "Instrumentation for Study of Biological Rhythms," FIRL Report F-B2029, 29 October 1962 - 30 November 1964, Volume I.

5-4. R. J. Gibson, Jr., R. M. Goodman, M. H. Halpern, and A. Marmarou, "Instrumentation for Biological Research," FIRL Report F-B2299, 9 November 1964 - 31 March 1966, Vol. II.

5-5. "Frequency Deviations in Wien Bridge Oscillators," Technical Staff Writer, Electronic Design News (EDN), January 1963.

5-6. Siliconix Inc., Application Note, "Low Pinch-Off Voltage Field-Effect Transistors, May 1963.

5-7. Siliconix Inc., Application Note, "Tetrode FET Characteristics," November 12, 1964.

6.0 DEEP BRAIN PROBES

6.1 THE SYSTEM

It was desired by Dr. M. Baldwin of NIH to ascertain deep brain temperature from primates and possibly humans during hypothermia. Because of the nature of the biological study it was considered important to observe brain temperature well before, during and for a period of time following hypothermia.

Since one of the conditions of the study required that the subject be ambulatory, it was clear that a telemetric system was necessary.

In general, the required system consisted of the following:

a. Fully autoclavable brain temperature-probes in three sizes: 1.5, 2.5 and 3.5 cm (penetration depth)

b. A small telemeter to be attached externally to the subject. This unit must be capable of accepting temperature sensor (probe) input and transmitting the information in coded form for distances of about 15 to 20 meters.

c. A receiver-recorder console capable of acquiring the transmitted signal from the telemeter and presenting in recorded format (analog) a linear record of brain temperature in either of two selected ranges:

(1) 15 - 40°C

(2) 35.5 - 38.5°C

Fig. 6.1-1 is a representational diagram of the complete system.

6.2 THE TEMPERATURE PROBES

Prior to the final selection of materials considerable discussion was held with Dr. Baldwin of NIH, Dr. Weatherby of PHS and Mrs. Lamberti of Dr. Baldwin's team, concerning the requirements for probe sterilization. It was decided unanimously that the only sterilization technique adequate for the application would be autoclaving. This meant that the complete probes must withstand temperatures on the order of 250 - 270°F and pressures of 15 to 30 psi for appreciable time periods.

The requirement for autoclaving imposed severe materials limitations for us in the probe design. The materials problems were finally overcome with the cooperation of our FIRL Chemistry Department, Mr. David Wix of the PENNtube Plastics Company of Philadelphia, the Dow Corning Company, and Emerson and Cumming, Inc., of Massachusetts. Detailed discussion materials will follow.

The mechanical design of the probes had, necessarily, to be related to the surgical procedures involved. For example, when a probe is to be applied, the scalp is laid back from the skull bone, a lead hole is drilled through the bone, and the hole is shaped with a burr tool. This results in a cavity in the skull bone of predetermined shape. It also exposes a small area of the dura. The dura is punctured, the probe emplaced with its base seated in the cavity made with the burr. The probe base is then sutured to the skull bone. It is

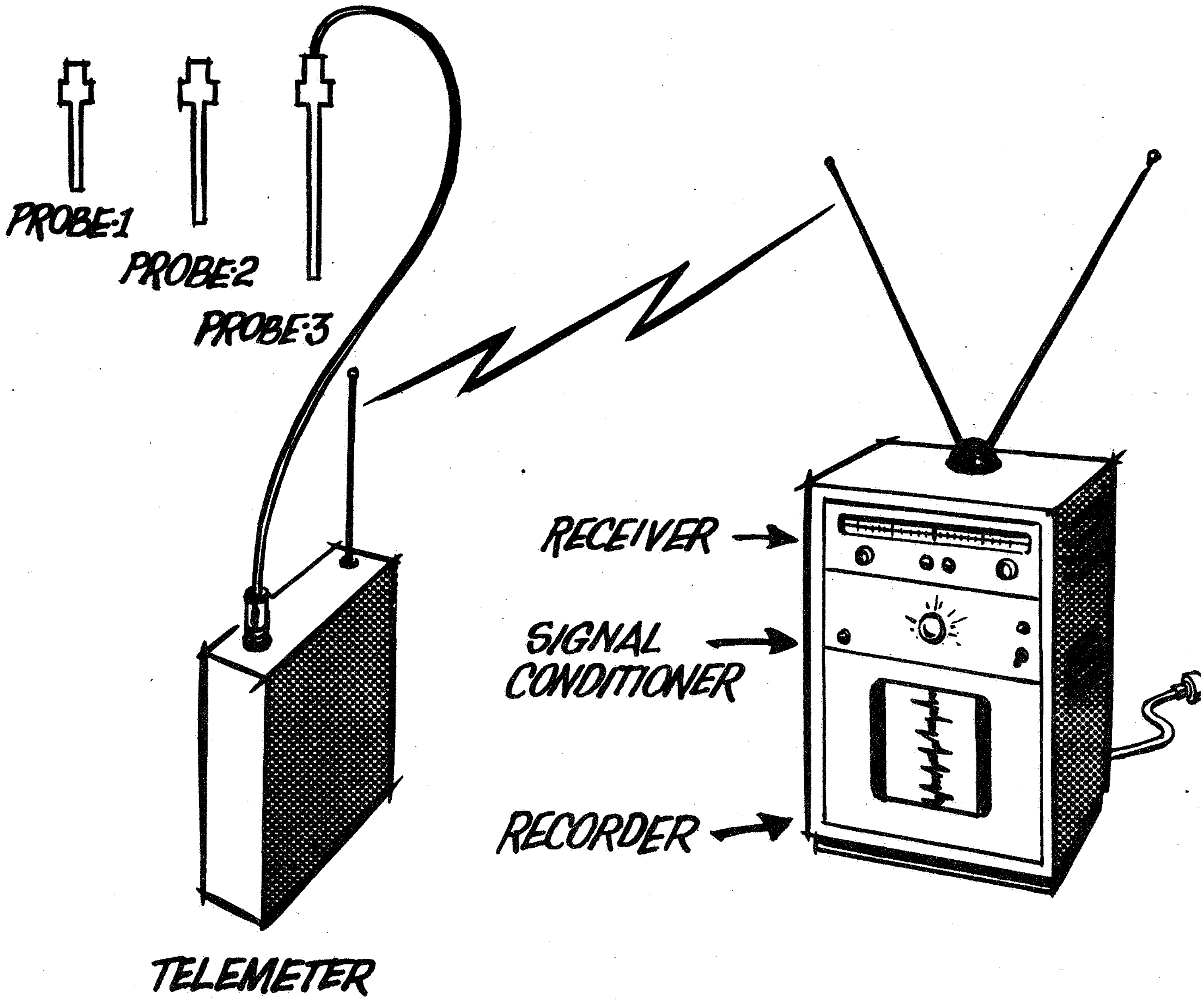

Fig. 6.1-1 Brain Probe System

clearly imperative that the proximal end of the probe not move after insertion. These procedures and requirements resulted in the design sketched in Fig. 6.2-1.

Fig. 6.2-2 illustrates the materials used in the probe construction and Fig. 6.2-3 is a photograph of a finished probe. Note that FEP Teflon was selected as the main probe tubing. One end was heat-sealed by the tubing manufacturer and cut and shaped by us. A .013" thermistor was inserted, and the probe tube assembly completely filled with silastic and cured. The tube assembly was then molded into the hard epoxy anchor base along with the stainless steel wire suture anchor. At the time of tube assembly the safety-tension connector was sealed and connected in place.

It should be noted that the safety-tension connector represented a problem in the evolution of the probe. In the first place, no commercially available connector of sufficiently small size and with the safety-disconnect feature was available.

We designed the connector and built it using German silver and polyphenylene oxide. These materials performed admirably in all respects other than fragility due to size.

After complete curing of the assembly, the probe anchor base was treated with primer and covered with a thin layer of medical silastic. Note that the anchor base was formed in a mold designed to fit exactly the burr hole of the skull.

A first experimental unit was fabricated and sent to Dr. Baldwin for culture studies to be processed after autoclaving. Results were entirely satisfactory.

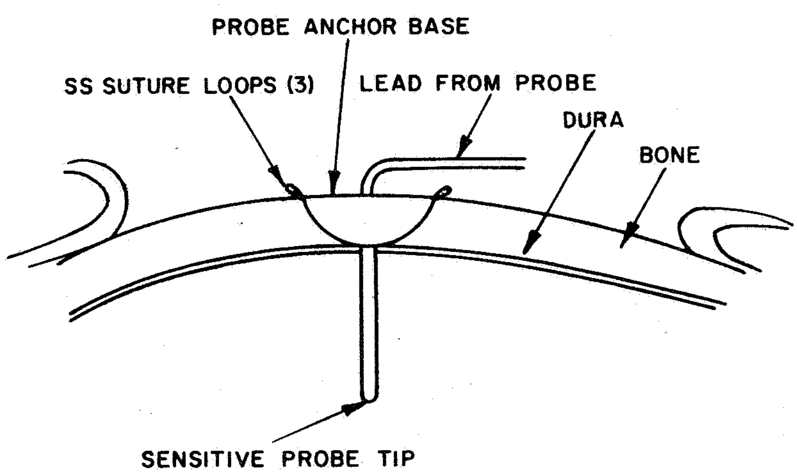

Fig. 6.2-1 Brain Probe Sketch

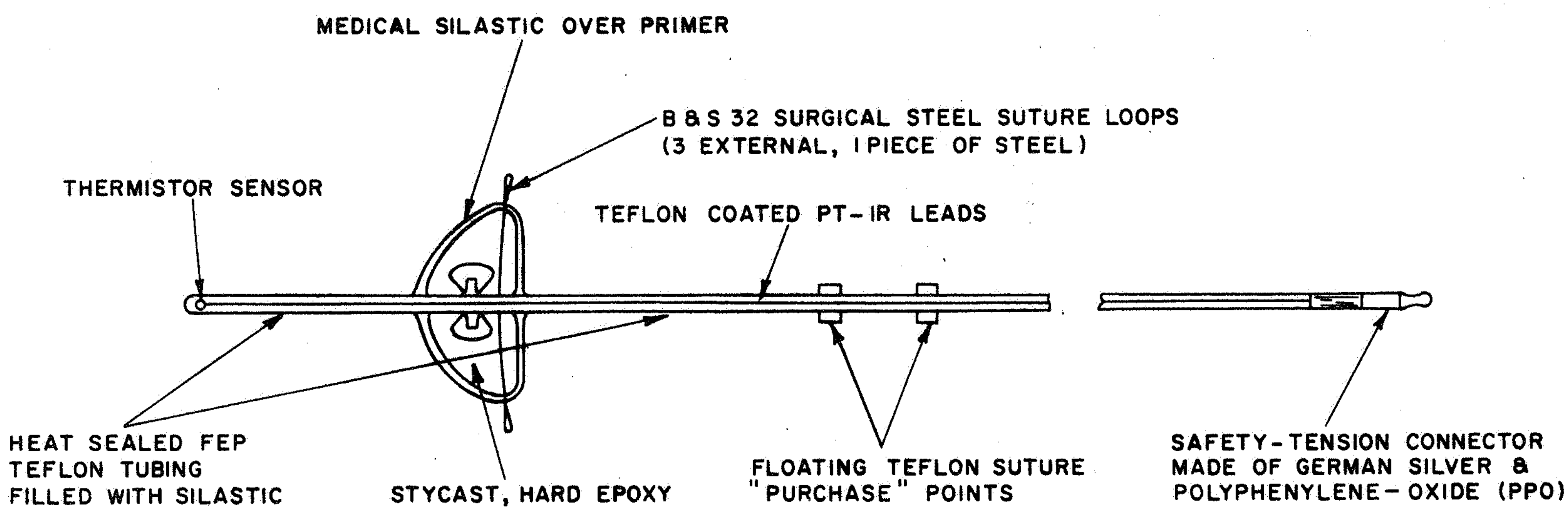

Fig. 6.2-2 Probe Construction

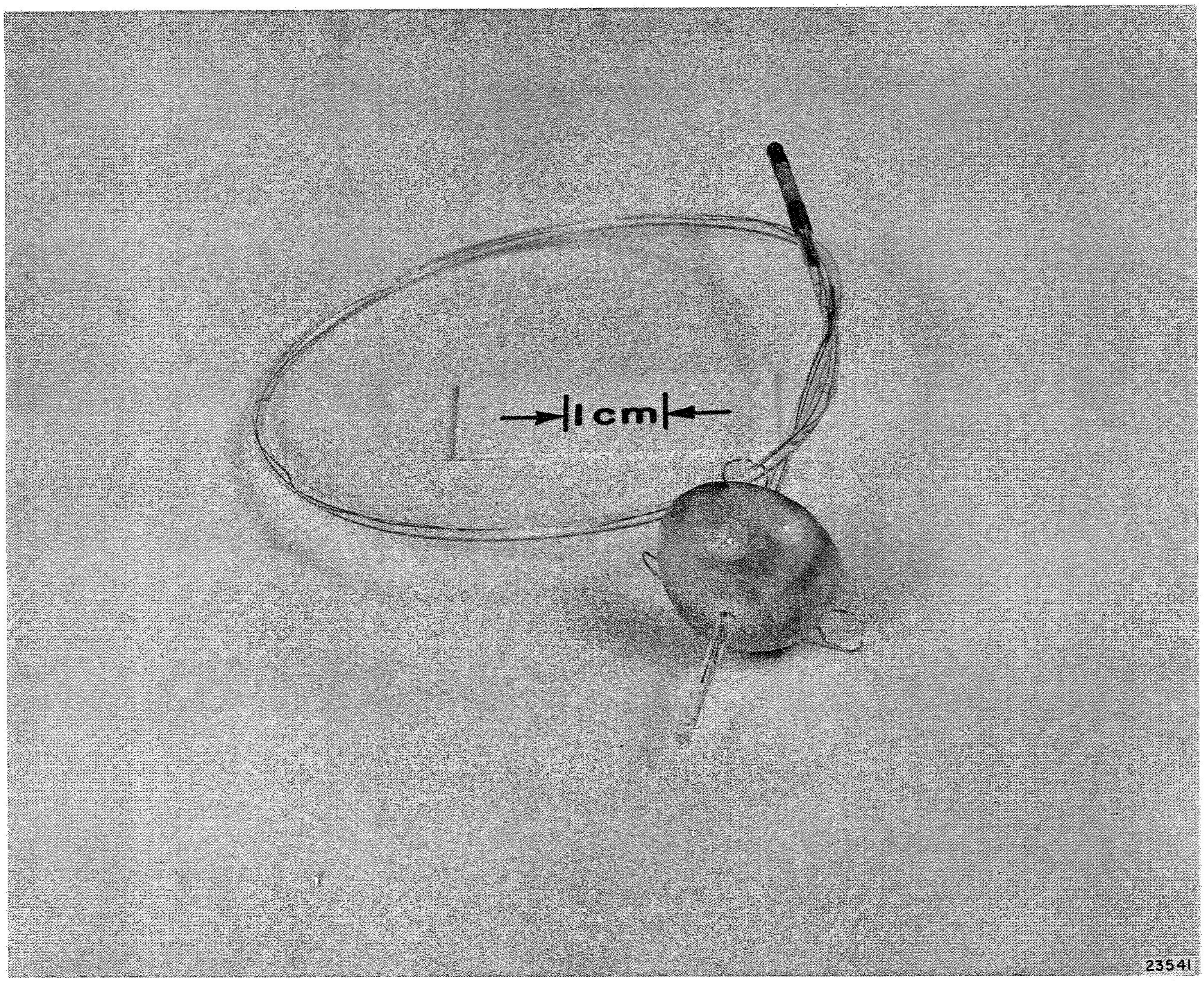

Fig. 6.2-3 Brain Probe

Three probes of the desired characteristics were made. It must be noted that in the thermistor size required, absolute curve matching was not available from thermistor to thermistor. This characteristic was taken into consideration in the design of the console signal conditioner.

The thermistor used was a VEECO unit, type 61A8.

6.2.1 Experience and Future Plans

The first-generation probes described above were evaluated in the operating room. It became clear that the distal section of the probe tube had to be grasped forcibly to feed it under the scalp and out of a small incision at the neck. This technique produced severe stresses on the safety-tension connection, which is too fragile for such handling. The situation could be ameliorated by first feeding a hollow Teflon catheter over the desired path, inserting the distal end of the probe tube through the catheter, and then withdrawing the catheter via the exit incision. Such a technique will no doubt, be attempted in the future. However, the safety-tension connector proved to represent an over-design in safety with a resultant probability of frequent disconnects.

In the future, distal probe tubes will be made of silastic tubing (medical grade), filled with silastic and firm contact rings for connection. This section of the probe will be very rugged indeed and, in conjunction with the catheter technique, is expected to be able to withstand the rigors of the OR and to perform satisfactorily.

6.3 THE TRANSMITTER

In order to realize substantial economy in the system a commercially available fm-microphone was used as the telemetering transmitter. The unit used is shown in Fig. 6.3-1.

This unit contains a built-in "marker signal" generator so that the user can locate himself in the fm band with the aid of an audible signal picked up by a standard fm receiver. The marker signal transmission was effected by push-button control and a simple unijunction transistor oscillator built into the transmitter.

We modified the transmitter so that it was able to accept variable resistance (the thermistor) as an input which in turn, modified the oscillation frequency of the internal marker-signal generator. In this simple manner we were able to transmit an fm signal, bearing a modulation frequency proportional to probe temperature, for substantial distances.

The transmitter utilizes an 8.6V mercury battery and has a useful operational lifetime of about 100 hours.

6.4 THE RECEIVER-RECORDER CONSOLE

Fig. 6.4-1 shows a photograph of the console. Starting from the top of the photograph the following components and functions are involved:

a. "Rabbit-ear" Antenna

This is used to pick up the transmitted signal and proved adequate in capability for the purpose at hand.

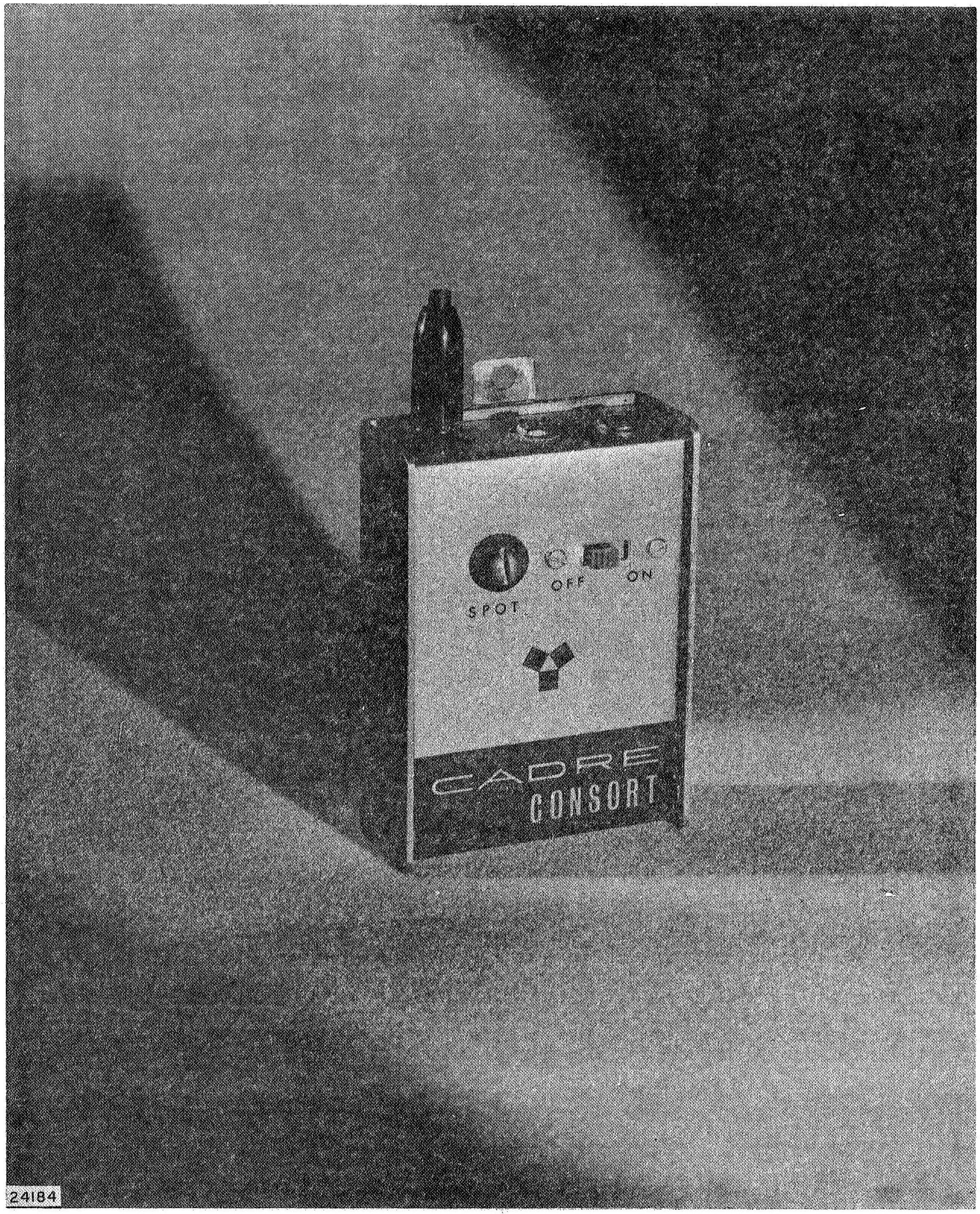

Fig. 6.3-1 FM Microphone

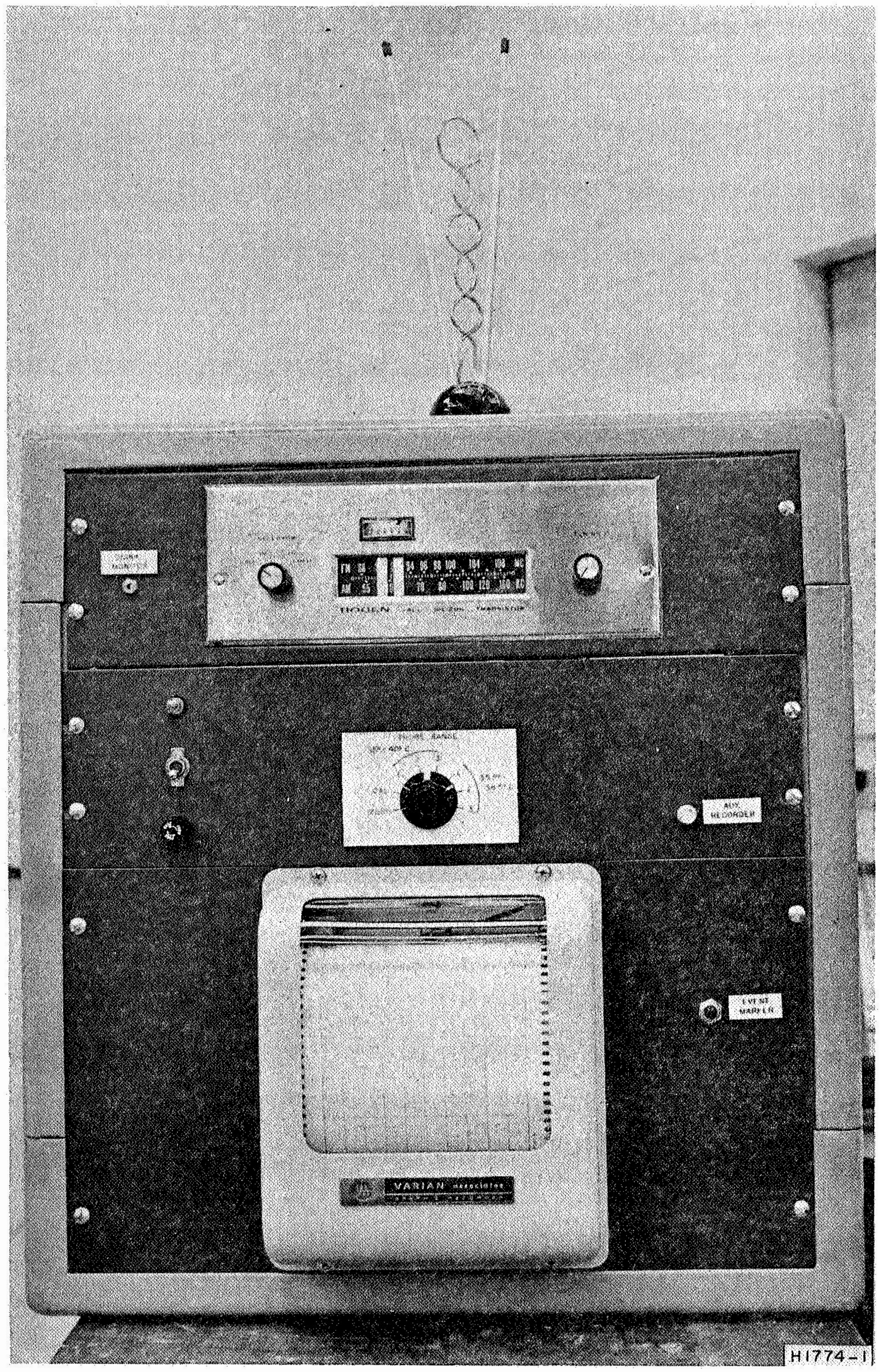

Fig. 6.4-1 Receiver-Recorder Console

b. The fm Receiver

This receiver permits detection of the signal modulation of interest. It contains automatic frequency control (AFC) circuitry and proved generally excellent for the purpose at hand. Its tuning meter permitted optimal tuning of the receiver for the telemetered signal. Since no loud speaker was desirable we incorporated audio signal monitoring via a headphone jack (seen at the left side of the receiver panel). A set of ultra-light-weight stethoscope type earphones was supplied with the unit.

c. The Signal Conditioner

This unit contained all the key controls for the Receiver-Recorder Console. Power control and indication are on the front panel. An auxiliary recorder output plug is supplied. Controls permit selection of:

> Zeroing of the recorder pen
>
> Calibration of the recorder gain (full scale)
>
> Switching to any of six circuits, pairs of which are related to each of the three probes supplied.

These conditioning circuits accomplish the following:

(1) For each probe there is a circuit to accept frequency modulation information (proportional to temperature in the 15° - $40^{\circ}C$ range), process it via a solid-state segmented linearization network and produce a 0-100 division linear drive for the recorder. Over the

15° - $40^{\circ}C$ range linearity is held to ca. 1.0% and a maximum error of ca. $\pm$.$2^{\circ}C$ may occur at the low end of the temperature range. It must be remembered that no two of the thermistor probes are absolutely identical. The data given above represents the worst case.

(2) For each probe there is a circuit to accept frequency modulation information (proportional to temperature in the 35.5 - 38.5 biological range), process it via a segment solid state active linearization network and produce a 0-100 division linear drive for the recorder. Over the 35.5 - $38.5^{\circ}C$ range, linearity is held to ca. 1.0% and a maximum error of ca. $\pm$.$18^{\circ}C$.

d. The Calibrator (not shown)

The calibrator is a small box containing three settable variable resistors locked at values equivalent to probe values for $37.0^{\circ}C$. This calibrator box is used for fast adjustment of the recorder pen deflection equivalent to a $37^{\circ}C$ input from any of the probes.

e. The Recorder

We selected the Varian G-11A recorder as a trouble-free simple unit. It is a potentiometric unit with built-in zener reference.

Initially we had considered the use of inkless recording, but were not satisfied with the trace legibility.

Two chart speeds are supplied: 12-inches/hour and 3-inches/hour. The former permits adequate high speed temperature vs. time discrimination with 1-inch/5minutes of travel. At this high speed of recording, one roll of paper will last for $3\frac{1}{2}$, 24-hour days. The low speed recording will permit the researcher to view a 24 hour record in six feet of paper. At this latter speed, a single roll of chart paper will last for 14, 24-hour days.

7.0 MARK IV IMPROVEMENT PROGRAM (AM TELEMETER)

For an extended period of time we have been observing the operation of implantable telemeters of the Mark IV type. Numerous changes in design have been incorporated by us to improve the compatibility of the basic circuit with low-drain, stabilized mercury cells.

For the most part, units of the "hamster" type, i.e., $1\frac{1}{2}$ cc, 3 - 4 grams, have performed admirably. As a matter of fact, eleven such units originally fabricated for the Ames group, are being observed by us—and are still operating some 19 months later.

It can be stated unequivacably that the Mark IV-D types and variations on that type have performed very well indeed.

However, our concern has been with the smaller units of the perognathus or "PLL" types. Performance has been spotty. In certain cases, computed lifetimes have been attained (4 - 7 months). In many cases failure occurs within 2-10 weeks of implantation. Detailed study indicates that failure is directly related to cell performance and not to circuit design. Meticulous unit dissection has indicated cell electrolyte leakage in many cases as well as cell gassing.

Schemes are being developed to evaluate cell batches as they are purchased in an attempt to remove cells expected to fail on implant. At the same time we undertook to improve the circuit design of the miniature implant in order to realize further cell current economy and improved energy distribution in the transmitted signal—both matters of considerable consequence to the biological investigator. The former means longer operational life, and the latter means the possibility for improved receiver equipment design.

We have succeeded in reducing current consumption to the order of $< 5 \times 10^{-6}$ amperes at $37^{o}C$, which means an anticipated lifetime of more than 7000 hours (almost 10, 30-day months) with ordinary WH-1 cells and 10,000 hours with improved cells. A new cell which would require slight increase in size and weight (ca. 0.3 gram) for the PLL implants would double these figures.

Of equal importance are construction changes made to improve the energy distribution in the transmitted signal. Fig. 7.0-1 (a,b) illustrates what has taken place. 7.0-1 (a) is a photograph of the frequency spectrum of a transmitted pulse from an old style "PLL" unit. Photograph 7.0-1(b) shows the distribution of a new unit. Even though the new units use less average current, the peak transmitted power is similar to that of the older units.

A number of these new units are being made up at this time. Units will be given to Drs. Halberg and Pittendrigh for their evaluation and to the personnel of the Biosatellite Project at Ames Research Center.

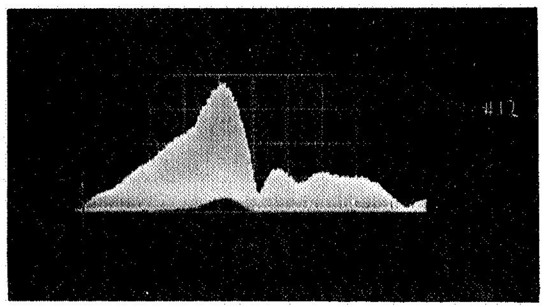

(a) Transmitted Spectra from MK IV PLL Unit

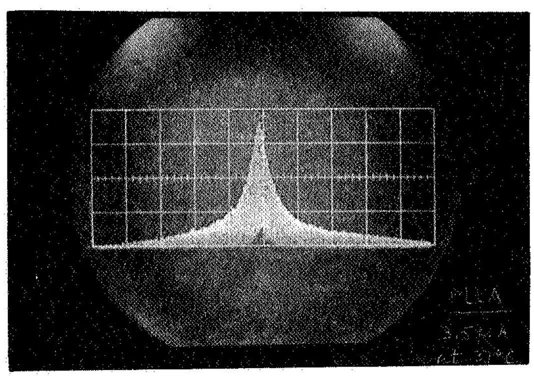

(b) Transmitted Spectra from MK IV PLLA Unit

Fig. 7.0-1 Telemeter Transmitted Pulse Spectra

8.0 COMMUNICATION AND COOPERATION

During August 1967, the authors attended the Seventh International Conference on Medical and Biological Engineering in Stockholm. R. M. Goodman presented a paper on multichannel implantable telemeters: "Simultaneous, Multi-Parameter Data from Implantable Telemeters."

8.1 VISIT TO HOLLY HILL LABORATORY OF THE MEDICAL RESEARCH COUNCIL, LONDON

Through the good offices of Mr. Heinz Wolff, Director of the Laboratory (MRC) the authors were able to spend a full day with his key personnel. We were welcomed by Mr. Henry Light, the Deputy Director and given an overview of their work. We then had the opportunity for detailed discussions.

We had for some time been in letter communication with Mr. Cliveden Weller of MRC. In his laboratory we were able to exchange directly information of considerable mutual interest. His experience with FET's led us to their use in our new SCO designs. Our experience with newly available microminiature components has already aided him. If we had accomplished no more than our extended conversations with Mr. Weller, it was worth the entire trip.

We also discussed philosophies, techniques and approaches to the problems of automatation in the hospital.

8.2 COOPERATION WITH DR. RONALD BARR, UNIVERSITY OF MISSOURI

Professor Barr of the Nuclear Reactor Facility, Space Sciences

Research Center, University of Missouri, is planning to read deep body temperature of rodents being subjected to a range of ambient temperature and simultaneously to various levels of hard radiation.

We discussed with Dr. Barr the application of implantable telemeters to his study. We agreed mutually that it was essential to determine the effects of hard radiation on the performance of the telemeters prior to their application in an animal study. Dr. Barr has agreed to subject three newly constructed Mark IV type units to hard radiation. We have agreed to fabricate four such units, calibrate and measure them carefully before the tests, hold one at the Laboratories for comparative purposes and ship three to Missouri for radiation exposure.

Figure 8.2-1 shows frequency spectra run on the units and 8.2-2 to -5 inclusive are temperature calibrations.

It is our agreed intent to publish jointly whatever useful data results from this exercise since the findings may prove of value to any researcher planning to use implants in animals to be exposed to hard radiation.

8.3 PLANNED PAPERS

A "Note" is planned on the work on the orientation response of Planaria maculata to the diminished magnetic field. The authors will be R. J. Gibson, Jr. and I. R. Isquith.

A paper is in preparation on MET; author is R. J. Gibson, Jr. A paper is in preparation on implantable telemetry in the study of ovarian function. Authors are H. Balin and R. M. Goodman.

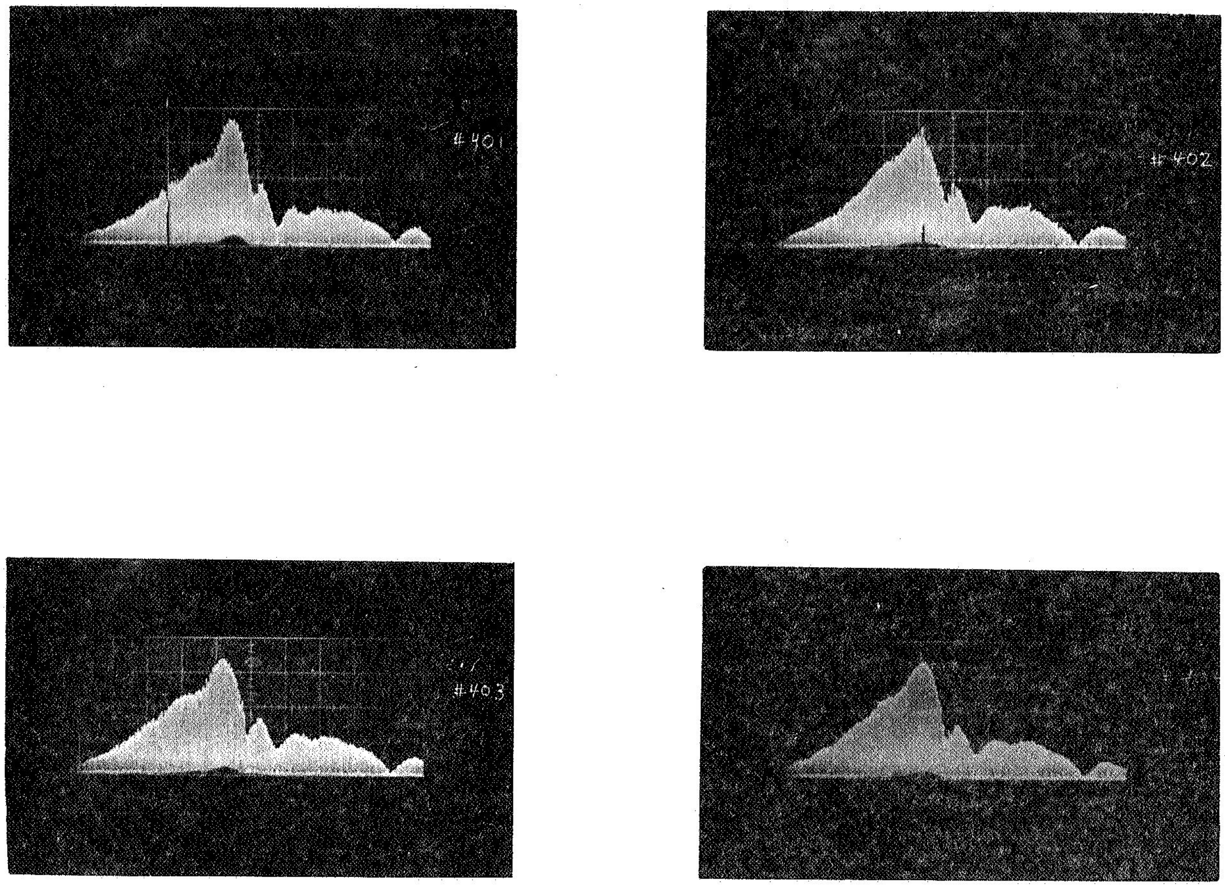

Fig. 8.2-1 Photo, Transmitted Frequency Spectra for U of Mo. Units

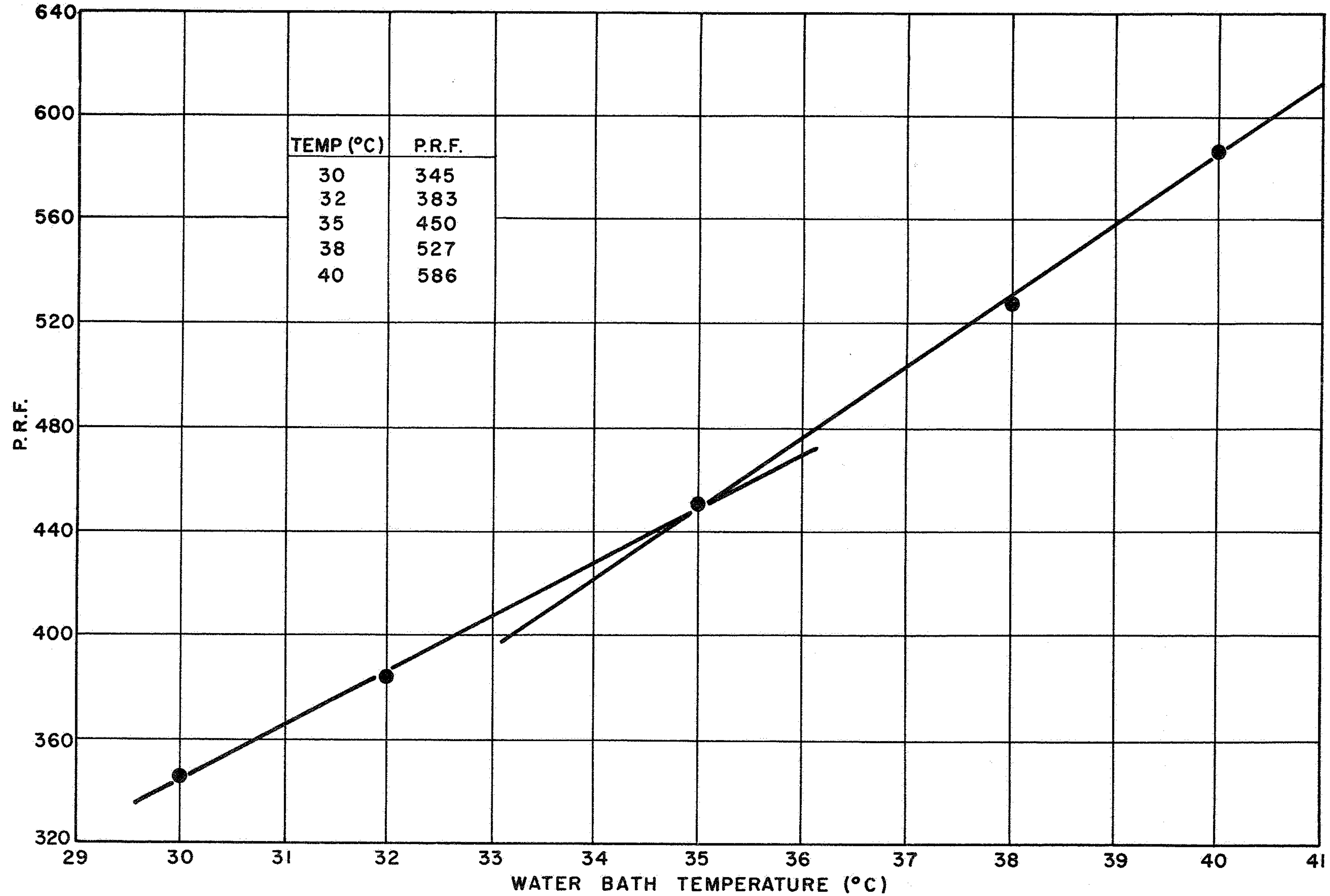

Fig. 8.2-2 Calibration, Implant SN401

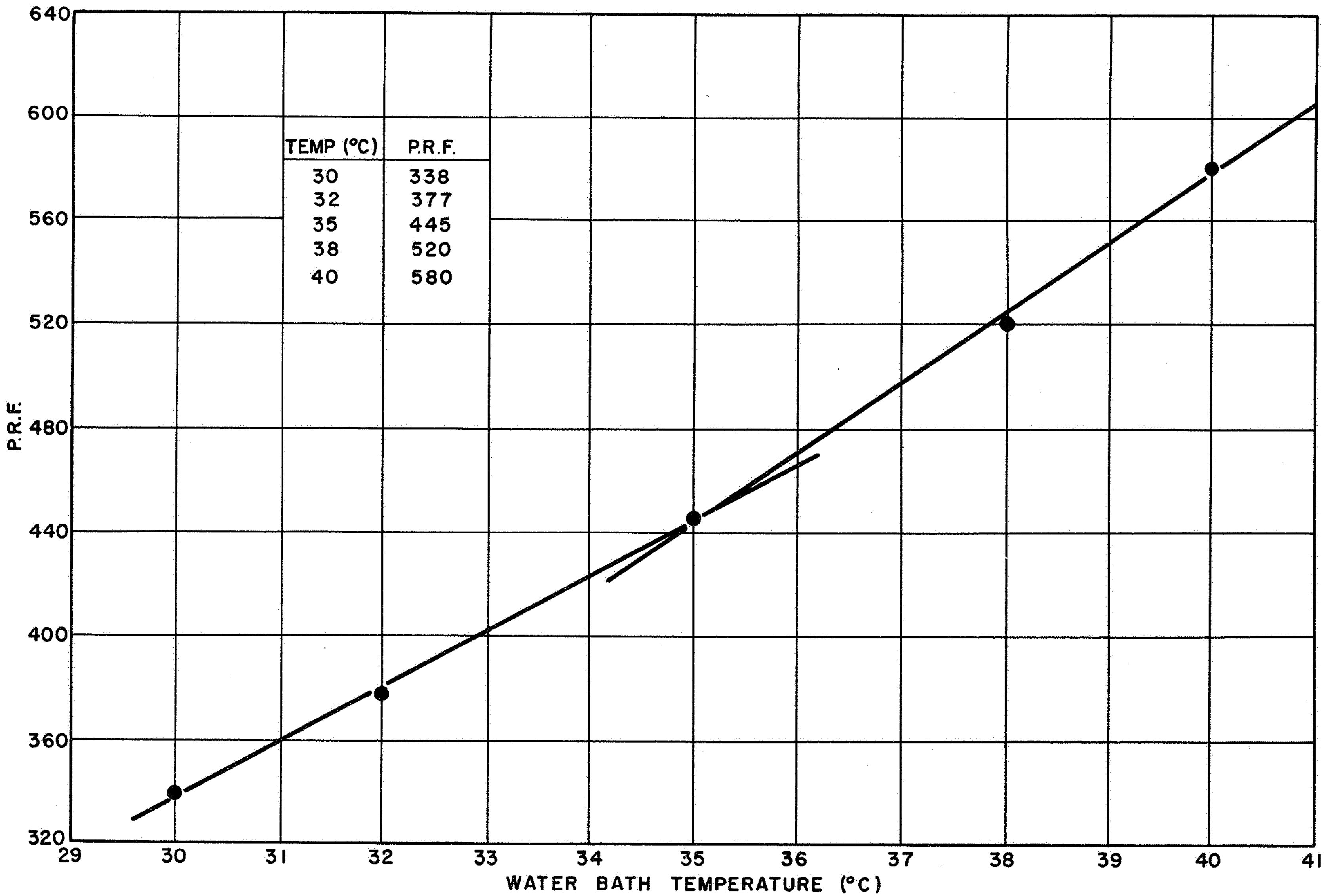

Fig. 8.2-3 Calibration, Implant SN402

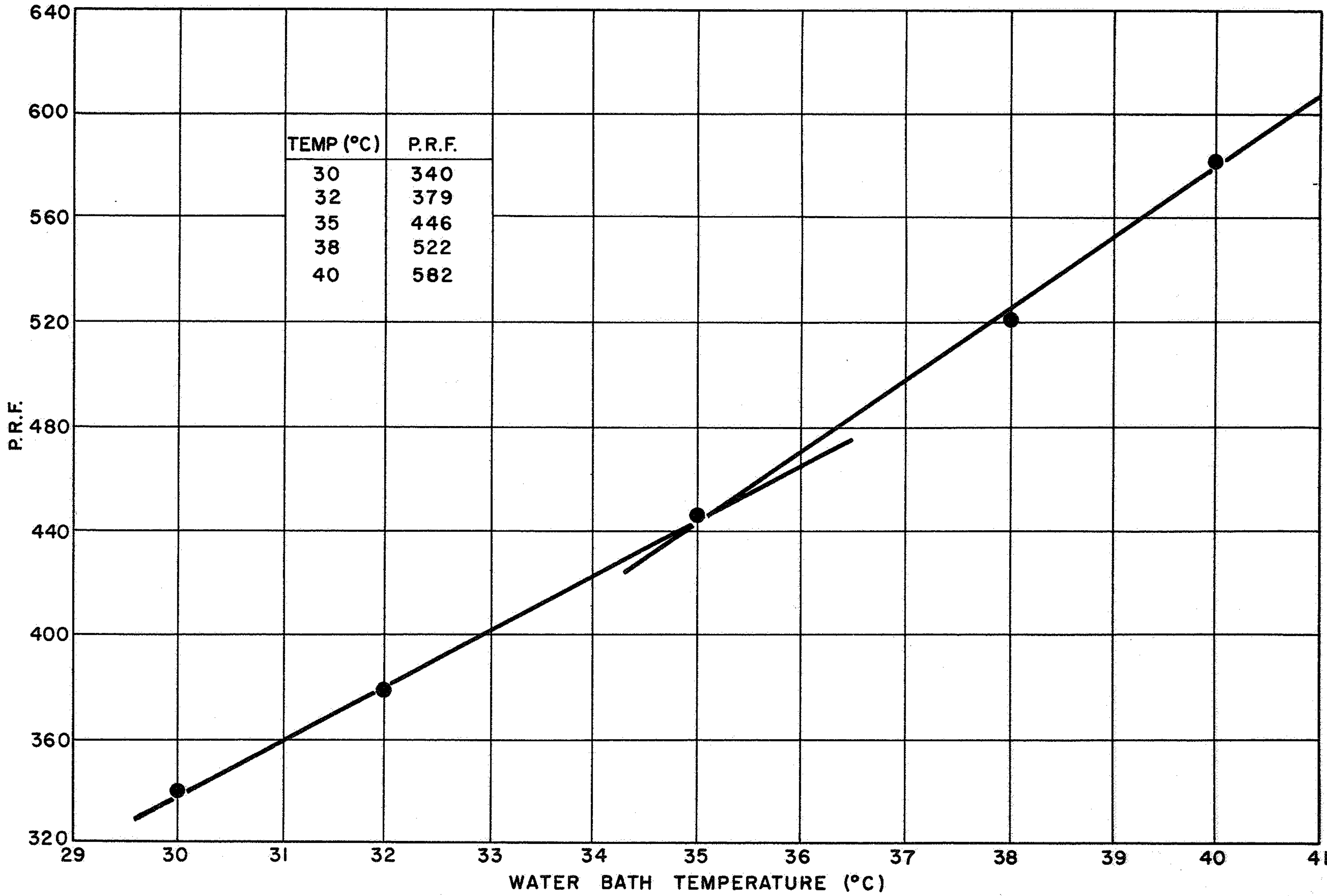

Fig. 8.2-4 Calibration, Implant SN403

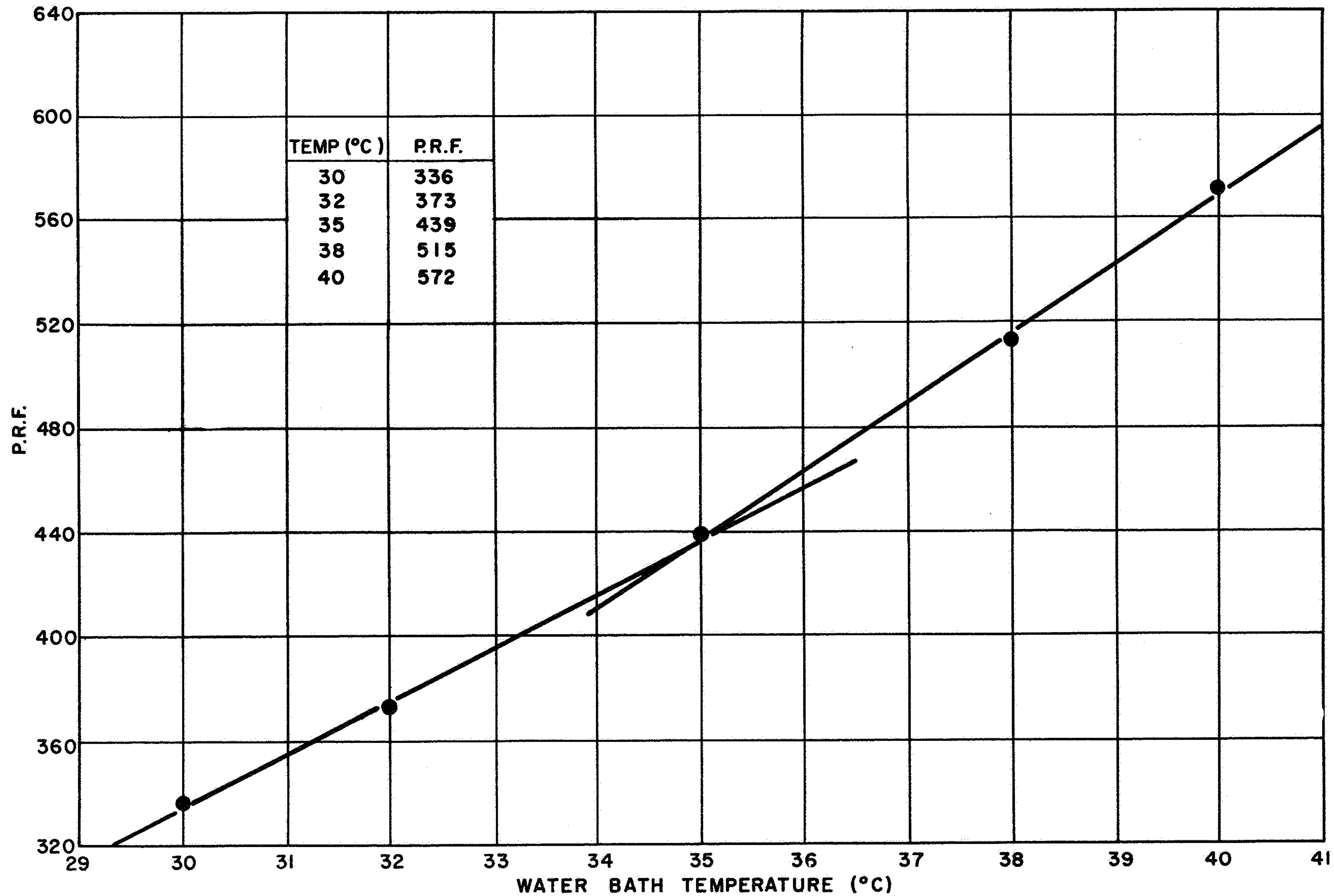

TEMP (°C)	P.R.F.
30	336
32	373
35	439
38	515
40	572

Fig. 8.2-5 Calibration, Implant SN404

9.0 MAGNETIC FIELDS FOR BIOLOGICAL EXPERIMENTS

One of the sizeable problems facing biologists who wish to perform experiments in a magnetic field is the production of that magnetic field. In order to perform a meaningful experiment, the magnitude, direction and uniformity of the field should be known for the region or volume in which the biological materials will be placed. For fields on the order of the earth's field, shields of high permeability or air core coils are suitable. For fields greater than 100 gauss and of any extent it is generally necessary to utilize iron core coils or permanent magnets. But for fields between one and 100 gauss and values in the range of zero to a 10^6 cubic centimeters air core coils are most suitable and practical. Many biological specimens and systems from bacteria and protozoa to small unconstrained mammals as well as a large variety of botanical specimens can be readily accommodated in air core coils producing fields of less than 100 gauss.

While it is practical and not expensive to produce coils for these conditions, it is difficult and expensive to determine and design coils to give the desired volume with specified magnitude, direction and uniformity of field.

In the past, several well-known relationships for standardized configurations have been available, but no simple general procedure for calculating the fields has been available.

These standard forms are the long solenoid, single flat coil, Helmholtz coils and Ruben's Cube coil, (9-1, 9-2). Barker (9-3, 9-4) has also described a configuration utilizing three coils for producing a uniform magnetic field and has gone to considerable pains to include such practical matters as insulation thickness and packing factors of the wire, but his method of calculation is limited to one specific configuration and is rather elaborate requiring much computation and iteration. These configurations are not always suitable for space or convenience reasons, and it would be most useful to have a simple means of calculating the magnetic field for the general case. For example, the simple case of two coils spaced one diameter apart instead of one radius apart and taking into consideration the finite size of the windings is, while simple in geometry, difficult to calculate except along the axis of symmetry. Approximate methods, evaluation of integrals and/or infinite series etc. are necessary. Blewett (9-5) has given tables and approximate methods, but the tables do not extend even to the case of coils spaced one radius (Helmholtz coils) let alone to those spaced two radii apart. His approximate methods of calculation require the use of tables of K & E, the complete elliptic integrals with modulus k^2, which in general are not available to the degree of tabulation desired. Dwight (9-6, 9-7) and Dwight and Peters (9-8) in a series of papers have exhaustively treated the cases of cylindrical coils with results requiring the use of surface zonal harmonics in the summation of one or a series for each point in the field desired. While formally the problem is solved, it is most time consuming and subject to error because of the many numerical operations required.

Just this last year Hart (9-9) has published extensive tables (Universal Tables for Magnetic Fields of Filamentary and Distributed Circular Currents). This book of 489 pages has more than 90% tables and less than 10% explanation, and this ratio is indicative of the ease with which these tables may be used. Only a few steps of simple arithmetic are required to determine the magnetic field at a known position with respect to a single turn or coil of finite size. These tables were computed by means of a Univac 1108 and are far more extensive and of finer subdivision than any tables published previously. Any circular coil (or number of coils) configuration can be handled easily. For regions where the field is nearly uniform an accuracy of better than 0.01% is possible. Overall the accuracy is better than the accuracy to which the coil dimensions can be measured. Especially useful is the fact that distributed currents are included. This makes possible the accurate calculation of the fields from coils of finite and even large relative size. These calculations can be made for real coils with real dimensions with greater ease and accuracy than could previously be done for idealized coils. In addition, the radial field can be calculated with the same ease and accuracy as the axial field, on and off axis, an absolute necessity when trying to determine the uniformity of a field from any practical coils.

This set of tables is recommended to everyone concerned with this problem, even to those with a large scale computer and program available. The last line in the book testifies to the enormous number of calculations which are required for the accurate calculation of magnetic fields: ..."The final entry in Table 1-A, for example, consists of the summation of more than 2.7 x10^7 solutions of the basic equation..."

A calculation for two circular coils of reasonable dimensions separated by one coil diameter for several points between the coils is given in the following calculation. Calculations are made for these same two coils and the same points between them except that the coils are spaced as a true basic Helmholtz pair (spacing = one radius). This provides us with a useful comparison of how the uniformity of the field in a given region changes as the coils are moved apart.

Calculation of the field at several points by means of Hart's tables between two coils of practical finite dimensions spaced one radius apart (Helmholtz coils).

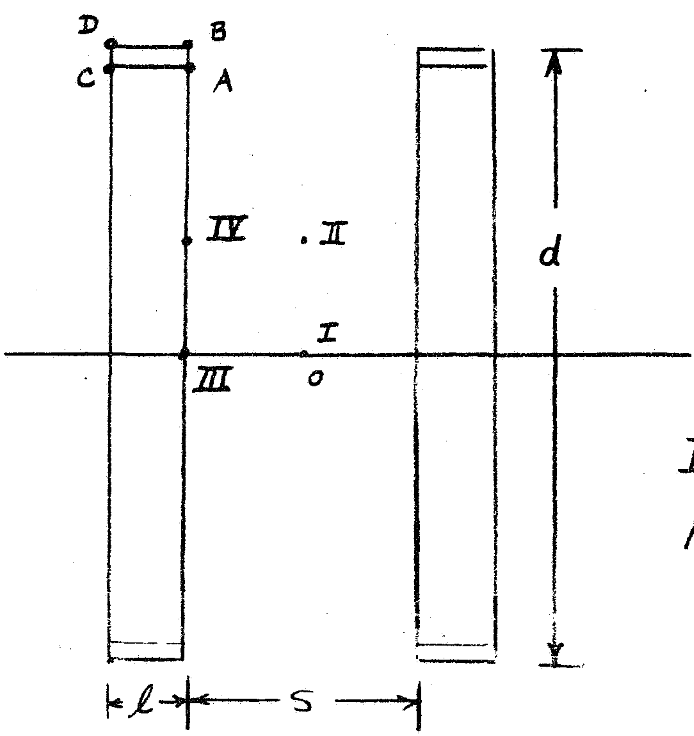

d = 50 cm. (coil dia.)

s = 20 cm. (coil spacing - inside)

ℓ = 5 cm. (coil length)

t = .090 cm. (coil thickness)

I = 1.0 amp. (current in coil)

N = 50 each (number of turns)

practical wire size # 19 enameled.

J = current density in coil = $N \frac{I}{A}$ = 109.65 amps/cm^2

Coordinates of points where field is calculated (origin at center of coil pair)

Point	Z	r = h
I	0	0
II	0	10 cm
III	10 cm	0
IV	10 cm	10 cm

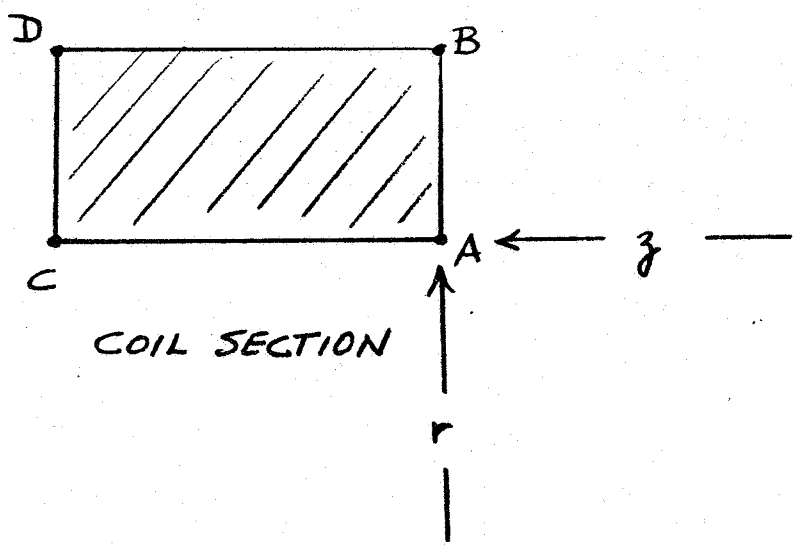

Z measured from points I through IV to corner points A through D. r measured from coil axis to points A through D.

Point II (s coil) d coil same by symmetry h = 10 cm

	Z	r	S_r	S_z
A	10	25.0	367.864	515.646
B	10	25.09	368.152	517.946
C	15	25.0	440.353	641.307
D	15	25.09	440.857	644.408

S_r and S_z values are combined to give $S'_{r \text{ or } z}$ values by

$S'_z = S_p - S_b - S_c + S_d$ (for z)

$S'_r = S_a - S_b - S_c + S_d$ (for r)

$$S''_z = 2S'_z = 2(.801) = 1.602$$

$$S''_r = S'_{rs} - S'_{rd} = .216 - .216 = 0$$

$$B''_z = 10^{-3} \; jhS''_z = 1.757 \text{ gauss}$$

$$B''_r = 10^{-3} \; jhS''_r = 0$$

Point IV (s coil)

	s coil				d coil			
	Z	r	S_r	S_z	Z	r	S_r	S_z
A	0	25.0	0	0	20.0	25.0	482.002	722.530
B	0	25.09	0	0	20.0	25.09	482.687	726.217
C	5	25.0	237.533	316.018	25.0	25.0	506.835	776.819
D	5	25.09	237.619	317.265	25.0	25.09	507.657	780.932

$$S''_z = S'_{zs} + S'_{zd} = 1.247 + .426 = 1.673$$

$$S''_r = S'_{zs} - S'_{zd} = .086 - .137 = -.051$$

$$B''_z = 10^{-3} \; jhS''_z = 1.834 \text{ gauss}$$

$$B''_r = 10^{-3} \; jhS''_r = .056$$

Points I and III are on axis points and are calculated somewhat differently:

$$B_z = 10^{-3} J \left[r_2 \left(T_d - T_b \right) - r_1 \left(T_c - T_a \right) \right]$$

B_r always 0

Point I - Values for both coils same at point I

	z	r	W	T
A	10	25.0	2.500	413.990
B	10	25.09	2.509	413.342
C	15	25.0	1.6667	483.977
D	15	25.09	1.6727	483.403

r_2 = outer radius = 25.09

r_1 = inner radius = 25.00

$W = r/z$

and $B_z'' = 2B_z' = 2\ (10^{-3})\ (109.65)\ (8.1555) = 1.788$ gauss

Point III

	(s coil)				(d coil)			
	z	r	W	T	z	r	W	T
A	0	25.0	0	0.000	20	25.0	1.2500	526.580
B	0	25.09	0	0.000	20	25.09	1.2545	526.095
C	5	25.0	5.000	290.590	25	25.0	1.0000	553.780
D	5	25.09	5.018	289.987	25	25.09	1.0036	553.390

$B_{zs}' = 1.2088$

$B_z'' = B_{zs}' + B_{zd}' = 1.739$ gauss

$B_{zd}' = 0.5298$

SUMMARY:

	B_z(gauss)	B_s(gauss)
Point I	1.788	0
II	1.757	0
III	1.739	0
IV	1.834	- .056

If point I is considered as the base point, then

Point II is 1.7% low

Point III is 2.7% low

Point IV is 2.6% high

Calculations of the field at several points by means of Hart's tables between two coils of practical finite dimensions spaced one diameter apart.

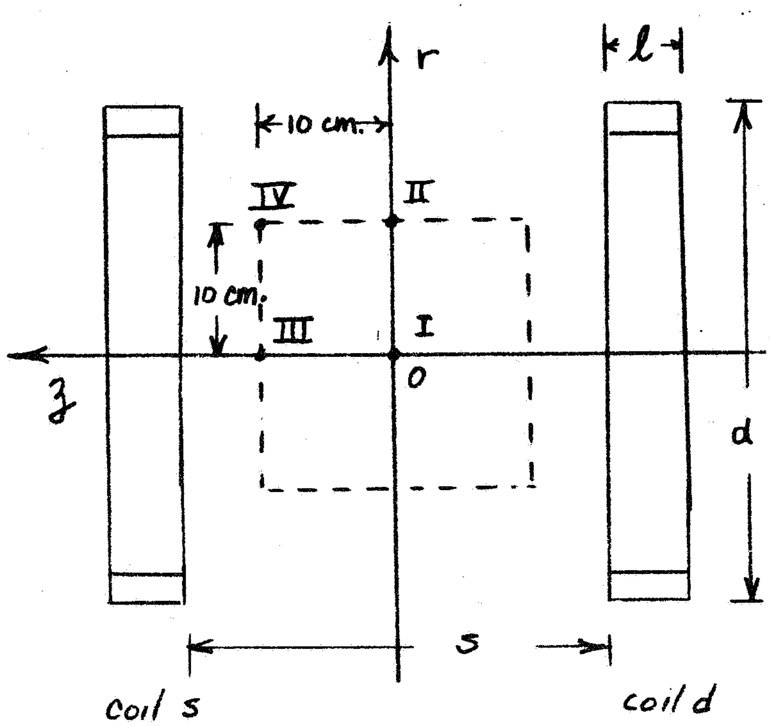

$d = 50$ cm (coil diameter)

$s = 50$ cm (coil spacing inside)

$l = 5$ cm (coil length)

$t = 0.090$ (coil thickness)

Current in coil 1.0 amperes

Number of turns 50 each

No. 19 enameled wire will give almost exactly 50 turns in 5 cm

Bare wire diameter .0359" nom. = 0.090 cm.

$$J = \text{current density} = \frac{\text{current (amps)}}{\text{area (cm}^2\text{)}} N$$

$$= N^1/.0912 \times 5 = 2.193 \text{ N amps/cm}^2$$

$$= 109.65 \text{ amps/cm}^2$$

(Hart Universal Tables, see 9-9)

Table I is used for points II and IV. Table II is used for points I and III. The calculations are slightly different for these two tables since Table I is for off axis points, Table II for on axis points.

Two calculations must be made for each point, one for each of the coils, s (left) and d (right). These must be combined so that the radial fields subtract and the axial fields add at each point.

Coordinates (Dimensional)of Points with Respect to Origin
z + to left - Origin at Center of Symmetry of Two Coils

I	z = 0	r = 0
II	z = 0	r = 10 cm
III	z = 10 cm	r = 0
IV	z = 10 cm	r = 10 cm

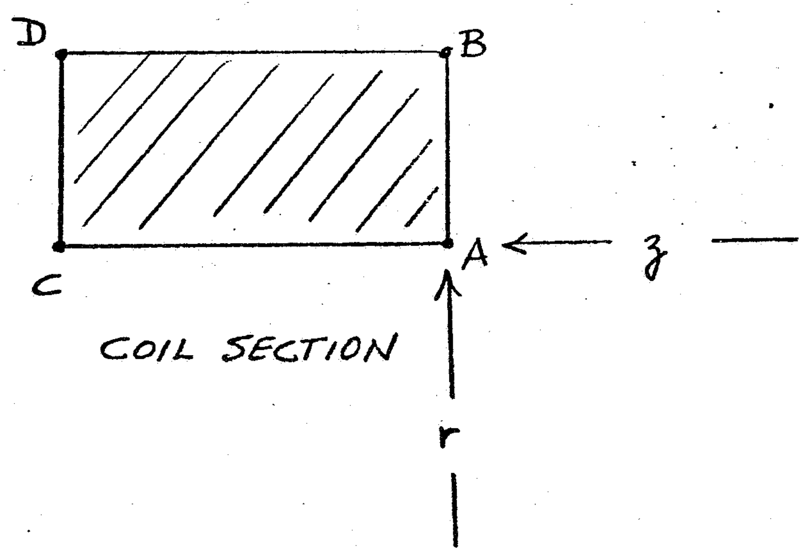

Z is measured from points I through IV to each of corner points A through D; r is measured from axis of symmetry to corner points A through D.

Point II (s coil) values for d coil same as s coil because of symmetry

	z	r	S_r	S_z	
A	25.0	25.00	506.835	776.819	
B	25.0	25.09	507.657	780.932	h = 10 cm
C	30.0	25.00	522.200	814.306	
D	30.0	25.09	523.121	818.732	

S_r and S_z values combined by following formula

$$S_z = S_a - S_b - S_c + S_d \text{ (for z values)}$$

$$S_r = S_a - S_b - S_c + S_d \text{ (for r values)}$$

For two coils (s and d)

$$S_z'' = 2S_z' = .626$$

$$S_r'' = S_{rs}' - S_{rd}' = 0$$

$$B_z = 10^{-3} jhS_z \qquad B_r = 10^{-3} jhS_r$$

For B_z = .6864 gauss

Point II B_r = 0 gauss

Point IV (s coil) h = 10 cm (d coil)

	z	r	S_r	S_z	z	r	S_r	S_z
A	15.0	25.0	440.353	641.307	35.0	25.0	532.049	840.971
B	15.0	25.09	440.857	644.408	35.0	25.09	533.041	845.631
C	20.0	25.0	482.002	722.530	40.0	25.0	538.572	860.452
D	20.0	25.09	482.687	726.217	40.0	25.09	539.614	865.289

Then

$$S_z'' = S_{zs}' + S_{zd}' = 0.763$$

$$S_r'' = S_{rs}' - S_{rd}' = 0.131$$

For

$B_z = 0.837$ gauss

Point IV $B_r = 0.144$ gauss

For Point I

r_2 = outer radius

r_1 = inner radius

$$B_z = KJ\left[r_2(T_d - T_b) - r_1 (T_c - T_a)\right]$$

$B_r = 0$

Point I (s and d coil)

	z	r	W	T	
A	25.0	25.0	1.000	553.7800	Using 5 point Lagrange
B	25.0	25.09	1.0036	553.3894	interpolation between
C	30.0	25.0	0.8333	571.8775	tabular values where
D	30.0	25.09	0.8363	571.5575	necessary

Then $B_z = 0.746$ gauss $B_r = 0$ (Point I)

For Point III

	(s coil)				(d coil)			
	z	r	w	T	z	r	w	T
A	15.0	25.0	1.6667	483.983	35.0	25.0	.71428	584.372
B	15.0	25.09	1.6727	483.400	35.0	25.09	.71685	584.115
C	20.0	25.0	1.2500	526.580	40.0	25.0	.62500	593.280
D	20.0	25.09	1.2545	526.095	40.0	25.09	.62725	593.058

Then $B_z = B_{zs} + B_{zd} = .8967$ gauss $B_r = 0$ (point III)

SUMMARY:

	B_z(gauss)	B_r(gauss)
Point I	.746	0.0
II	.687	0.0
III	.897	0.0
IV	.837	0.144

If point I is considered our base point,

then Point II is 7.9% low

Point III is 20.2% high

Point IV is 12.2% high

This can be compared to the values obtained for the basic Helmholtz arrangement previously calculated. We see that not only are the values of the field less than one-half those for the true Helmholtz separation, but that the variation or lack of uniformity is many times greater.

In a standard Helmholtz arrangement the field is uniform to ± 0.5% over a volume .0245 d^3. For the volume we have chosen (.064 d^3) or 2.6 times larger, the field is uniform to ± 2.65%. This may be a great advantage to the experimenter (in volume) with really little loss in uniformity of field. The ease with which the calculations can be made allows the experimenter to choose both the volume and uniformity required for his experiment and provides a freedom not hitherto enjoyed.

9.1 REFERENCES

9-1 Wolff, Norman, "The Applications of Magnetometers to the Dynamic Simulation and Control of the Geomagnetic Environment," Technical Paper, Vickers Inc., Division Sperry Rand Corp.

9-2 Rubens, S., "Cube Surface for Producing a Uniform Magnetic Field," Rev. Sci. Inst., Vol. 16, No. 9, 1945.

9-3 Barker, J. R., "New Coil Systems for the Production of Uniform Magnetic Fields," Jr. Sci. Instr., Vol. 26, 273-275, August, 1949.

9-4 Barker, J. R., "An Improved Three Coil System for Producing a Uniform Magnetic Field," Jr. Sci. Instr., Vol. 27, July 1950.

9-5 Blewett, J. P., "Magnetic Field Configurations due to Air Core Coils," Jr. of Applied Physics, 968-976, 18:1947.

9-6 Dwight, H. B., "The Magnetic Field of a Circular Coil," Philosophical Magazine, Vol. 11, 3948-3957, April 1931.

9-7 Dwight, H. B., "Formulas for the Magnetic Field Strength Near a Cylindrical Coil," AIEE Transactions, Vol. 61, 327-333, June 1942.

9-8 Dwight, H. B., and Peters, G. O., "The Computation of Magnetic Field Strength of Round Coils of Small Cross Section," AIEE Technical Paper 44-110, May 1944.

9-9 Hart, Philip J., Universal Tables for Magnetic Fields of Filamentary and Distributed Circular Currents, American Elsevier Pub. Co., 1967

10.0 MAGNETIC SHIELDING

The triple Mu-metal shields designed previously and used in the Planaria navigation study and in the Blepharisma growth studies have proved to be both useful and practical (10-1, -2, -3). They were light in weight, relatively inexpensive and when used in the horizontal (axis of cylinder) position yielded an attenuation factor of about 500 for the earth's field. When used in a vertical direction the attenuation was only about 100. In both orientations, however, the region of maximum attenuation was small. Some other shortcomings were also noted. The use of flat plates for end covers while inexpensive is not as satisfactory as would be the use of overlapping caps. Leakage was noted around the ends covered by the flat plates unless great care was taken to ensure that no gaps (even .010") existed between the cylinder and the end plates. A second shortcoming was that the Mu-metal while sufficiently thick for shielding purposes was rather weak mechanically. This can be corrected by using a foamed-in-place plastic filler between the three shields rather than using sections of plastic as inserts. The previous design was actually so weak that handling produced distortions in the shield which were reflected in the attenuation properties. As assembled, the three cylinders did not have their open ends in the same plane. The inner cylinder protruded beyond the middle, which in turn protruded beyond the outer cylinder. The amount of protrusion depended upon the thickness of spacer used on the closed end. Originally this was considered of small consequence in the shielding properties. After some consideration and many measurements of the field around the mouth of the cylinders, it is believed that a better design would be to have just the reverse configuration, that is an arrangement of the cylinders such that each outer one would overlap the next inner one by approximately 1/10 to 1/5 the cylinder diameter; this would enhance the shielding considerably. This is felt to be especially desirable when the shields are used at an angle to the magnetic field other than 90°. Such would be the case when used in a vertical position with open end upwards or downwards. An increase in the length to diameter ratio from $1\frac{1}{2}$ to 2 is also considered desirable as this would yield a larger region along the axis of minimum magnetic field and would also, it is believed, reduce the sensitivity of maximum shielding factor to the angle made with the magnetic field. This would be useful in either the horizontal or vertical position.

Some work has been done on programming the Wadey equations for the calculation of shield design on the Wang Loci IIa computer. Time has not permitted a test of these as yet. There is also some question as to whether this programming should be continued or whether a Fortran IV program should be written since the capacity of the Loci is limited, and the gain in calculation economy would not be great. A Fortran IV program could be used on the Sci-Tek Univac 1107, which has an input output terminal at the Franklin Institute Laboratories. There is no question that if several shields have to be designed it will be necessary to have some kind of computer assistance since the number of calculations required is rather formidable, and the chance for errors in the calculations is great and can be disastrous since the equations are recurrent, each approximation depending on the last.

It is recommended that a new shield design be carried out using the recommendations suggested above and that measurements be made on this sheild to confirm the predicted improvements. Some tentative dimensions are offered here.

PROPOSED TRIPLE SHIELD DESIGN

Mu-metal - .020" or .030" thickness

Length

inner - 12.0"

middle - 12.5"

outer - 13.0"

Diameter

inner - 6"

middle - 7"

outer - 8"

End caps - three, one for each cylinder to overlap 1" of cylinder side

Cylinders to be assembled with foamed-in-place plastic for separation and mechanical support

While this configuration is somewhat larger than the original design, it is felt that the attenuation factor will in practice be considerably better for any orientation and will have a larger useful region of low magnetic field. Once a completely acceptable configuration has been determined, scaling to larger of smaller size will not be difficult.

10.1 REFERENCES

10-1 Gibson, R. J., Goodman, R. M., Halpern, M. H., and Marmarou, A. Final Report F-B2299, NASA Contract NSR-39-005-018, Nov. 1964 - March 1966.

10-2 Gibson, R. J., Goodman, R. M., Isquith I. R., Annual Report A-B2299-1, NASA Contract NSR-39-005-018, March 1966 - March 1967.

10-3 Gibson, R. J., Isquith, I. R., Final Report F-B2375, NASA Contract NSR-39-005-20, July 1967.

11.0 STATISTICS

In the continuing study of the Information Flow Loop or Biological Experiment Design Diagram (11-1) two of the most important modes which must be considered are those termed "Experiment Design" and "Correlation and Data Processing." The first was discussed rather completely in 11-1. The second concept contains among many other ideas, the procedures of statistical analysis. There are many texts and tables available discussing both of these subjects, but a list of books found useful here and with which we are familiar is given below:

Fisher, R. A., The Design of Experiments, Oliver and Boyd, Inc., 1947.

Fisher, R. A., Statistical Methods for Research Workers, Hafner Publishing Co., 11th edition, 1950.

Arkin, H. and Coulton, R. R., An Outline of Statistical Methods, Barnes and Noble, Inc., 1939 and later editions (paperback).

Davies, O. L. (ed.) Statistical Methods in Research and Production, Hafner Publishing Co., 3rd edition, 1957

Davies, O. L. (ed.) Design and Analysis of Industrial Experiments, Hafner Publishing Company, 1954.

Hoel, P. G., Introduction to Mathematical Statistics, John Wiley and Sons, Inc., 2nd edition 1954.

Finney, D. J., An Introduction to the Theory of Experimental Design, University of Chicago Press, 1960.

Cox, D. R., Planning of Experiments, John Wiley & Sons, Inc., 1958.

Adams, J. K., Basic Statistical Concepts, McGraw Hill Book Company, 1955.

Guilford, J. P., Fundamental Statistics in Psychology and Education, McGraw Hill Book Company, 1965.

Beyer, W. H. (ed.) Handbook of Tables for Probability and Statistics, The Chemical Rubber Company, 1966.

Siegal, Sidney, Non-Parametric Statistics for the Behavioral Sciences, McGraw Hill Book Company, 1956.

Winer, B. J., Statistical Principles in Experiment Design, McGraw Hill Book Company, 1962.

Natrella, Mary G. (ed.) Experimental Statistics, National Bureau of Standards Handbook 91, August 1963.

Tate, M. W., Clelland, R. C., Non-Parametric and Shortcut Statistics, The Interstate Printers and Publishers, Danville, Illinois, 1957.

Batschelet, E., Statistical Methods for the Analysis of Problems in Animal Orientation and Certain Biological Rhythms, American Institute of Biological Sciences, Monograph 1965 (paperback).

Moroney, M. J., Facts from Figures, Pelican Books, Penquin Books A-236 1956 (or later) (paperback)

These texts cover a wide spectrum of ideas in experiment design and statistical data analysis. They range from elementary to the most advanced procedures. The Fisher books are general and are written by the dean of biological statistics. Both Davies' texts in the examples given are slanted strongly towards industrial applications, but the ideas are presented clearly and with the necessary qualifications. Arkin is a good, cheap handbook with good standard tables. Finney and Cox are quite good and fundamental in experiment planning but not easy to read. Hoel and Adams are both good standard basic statistics. Guilford, while not oriented to the biologist, has excellent discussion and examples of analysis procedures. The Beyer handbook has tables for the most sophisticated analysis or planning; a few of the tables are extremely useful and not readily available elsewhere. Other tables would probably never be used, very little theory or explanation is given. Natrella is a good handbook with cookbook procedures (and complete tables) for analyzing many situations. It covers both standard (parametric) and non-parametric procedures and has excellent discussions and worked-out examples of each type discussed. Tate and Clelland cover material similar to Natrella but is not a cookbook. Batschelet is in a class by itself in that it covers material difficult to find elsewhere which is as modern and complete. It is a must for any work in angular analysis. Many biological problems can be handled satisfactorily in no other way than by the methods set forth in this small text. Clear, well worked out examples and appropriate tables make this a highly recommended book. Winer is rather advanced and completely describes procedures and techniques for quite sophisticated analysis and design. Analysis of variances is thoroughly covered in almost all of its ramifications to analysis of data not just from a theoretical standpoint. Siegal is a unique book in its approach and explanation. It thoroughly discusses the value of non-parametric statistics and gives the limitations. It is especially good for data where the number of subjects is small or the assignment of a continuous interval measurement is impossible. This book is so clearly written and so careful of making explicit the requirements of limitations of each procedure that it is recommended without reservation for anyone. The inclusion of the term "Behavioral Sciences" in the title might make a biologist overlook it. This would be a pity. Moroney is popular and easy reading but is fundamentally accurate and most useful as an introduction. It is replete with worked out examples and full of explanations of them. It also is highly recommended as a survey of the value of statistics in analyzing data. It is not elementary, although the examples are simple. It includes both parametric and non-parametric statistics and points out the shortcomings and pitfalls of both. It was felt that a listing and discussion of this nature would prove useful to many experimenters, especially since several of the books mentioned might be overlooked by those interested specifically in biological applications. Alternate viewpoints as provided in these texts often will clear up perplexing problems encountered when only the viewpoint of a different discipline is known.

11.1 REFERENCES

11-1 Gibson, R. J., Goodman, R. M., Halpern, M. H., and Marmarou, A. Final Report F-B2299, NASA Contract NSR-39-005-018, Nov. 1964 - March 1966.

This report has been written by:

R. J. Gibson Jr

R. J. Gibson, Jr.

R M Good

R. M. Goodman

Approved by:

R M Good

R. M. Goodman, Manager
Bio-Instrumentation Laboratory

CWHargens

C. W. Hargens, Technical Dir.
Electrical Engineering Div.